The multiscale physics of cilia and flagella

William Gilpin[1,3]*, *Matthew Storm Bull*[1] *and Manu Prakash*[2,4]*

Abstract | Cilia and flagella are fundamental units of motion in cellular biology. These beating, hair-like organelles share a common basic structure but maintain widely varying functions in systems ranging from the isolated flagella of swimming algae to the dense ciliary carpets that pump fluid in the brains of mammals. Experiments and models have begun to elucidate the inner workings of single cilia as complex nonlinear oscillators, and the variety of hydrodynamical phenomena that result from beating dynamics. These results have shed light on complex locomotion strategies observed in single-celled microorganisms and collective phenomena observed in microbial suspensions. In animal systems, dense ciliary arrays exhibit a variety of emergent phenomena, including active filtration, noise robustness and metachronal waves. Surprising phenomena have been observed in neuronally controlled ciliary arrays, demonstrating the need for new physical models of cilia that include central control, defect dynamics and topology. We review the emergent physics of cilia across scales, starting from the microscale dynamics of single cilia, and then proceeding to microorganisms and animal systems.

Cilia and flagella are slender, hair-like structures that protrude from many types of cells. In many cells, cilia act as a fundamental unit of motion, serving as key organelles that convert chemical energy into mechanical work in the form of an oscillatory beating motion[1]. Believed to have emerged nearly a billion years ago as a characteristic organelle of the first eukaryotic cells[2], it is unclear whether the first cilia were motile or were, instead, non-beating 'primary' cilia, serving as elongated antennae for sensing chemical and mechanical gradients[3]. In present-day organisms, many motile cilia can both sense and actuate, regulating their beat cycle in response to chemical cues or mechanical and hydrodynamical stimuli[4–6]. Beating cilia manifest in surprising contexts, including the undulatory swimming of ciliates and plankton, the filter feeding and breathing apparatuses of marine invertebrates and the lining of brain ventricles and other animal body cavities[7,8].

We use the terms 'cilia' and 'flagella' interchangeably, because there is no intrinsic structural distinction between cilia and eukaryotic flagella. However, in practice, 'flagella' typically refers to sparse or isolated structures used by unicellular organisms for locomotion; by contrast, 'cilia' refers to extended groups that occur in many protozoans and animals. Flagella typically enable propulsion by driving fluid continuously in parallel to the flagellar axis, whereas cilia push fluid orthogonally to their axis (and tangentially to their attachment surface) in a pulsatile manner during their power strokes[7]. Despite their functional differences, cilia and flagella have identical ultrastructure and nearly identical composition, with a characteristic 9-fold symmetry suggesting a common evolutionary origin. Existing theories for the evolution of the first cilia range from an endogenous origin via condensation of cellular actin networks to an exogenous origin due to invasion of a virus with 9-fold symmetry[2] or symbiosis with a bacterium[9]. Regardless of their provenance, over the course of evolution, the structure of cilia, discussed below, has remained remarkably conserved, even as their function has varied. However, multiple theories exist regarding the precise mechanism behind their beating.

More detailed discussions of ciliary evolution, as well as further analysis of ciliary anatomy and ultrastructure, can be found in other reviews[2,3,10,11]. Here, we focus on how the same basic structures conspire across scales to produce a remarkable array of complex physical phenomena in biological and bio-inspired systems. We organize our review across scales (FIG. 1), starting with the coupled chemomechanical dynamics of single cilia and results describing ciliary beating as a nonlinear limit cycle. We then turn to the problem of interactions. We describe studies showing how pairs of cilia and flagella can transiently synchronize via hydrodynamic or direct mechanical coupling, and the implications of this phenomenon for understanding both the behaviour of swimming microorganisms and the properties of synthetic arrays of colloidal oscillators. We then turn to the 'large N' limit, discussing phenomena observed in large ensembles of coupled cilia that appear in many

[1]*Department of Applied Physics, Stanford University, Stanford, CA, USA.*

[2]*Department of Bioengineering, Stanford University, Stanford, CA, USA.*

[3]*NSF-Simons Center for Mathematical & Statistical Analysis of Biology, Harvard University, Cambridge, MA, USA.*

[4]*Chan Zuckerberg BioHub, San Francisco, CA, USA.*

**e-mail: wgilpin@fas.harvard.edu; manup@stanford.edu*

https://doi.org/10.1038/s42254-019-0129-0

Key points

- The complex beating dynamics of cilia can be modelled as noisy, nonlinear oscillations driven by coupled chemical, mechanical and hydrodynamical forces.
- Small numbers of coupled cilia can transiently synchronize and desynchronize in a manner analogous to that seen in classical studies of coupled oscillators.
- The synchronization dynamics of cilia may play a role in facilitating locomotion and navigation by single-celled microorganisms.
- Many animals have 'carpets' of densely packed cilia, which are used to pump mucous and other circulating fluids in the brain and lungs. The beating dynamics of these ciliary carpets exhibit physical phenomena that include travelling waves and topological defects.
- Neuronally controlled cilia in certain animal systems exhibit a rich, and understudied, set of dynamical phenomena, making their study a promising research direction.

Microtubule
A tube-shaped protein assembly found in the cytoplasm of many cells. Microtubules allow cells to maintain their shape and internal arrangements, and they can aggregate to form specialized structures, including cilia.

invertebrates and in the lungs and brains of mammals. We highlight the role of dimensionality in ciliary dynamics: single cilia serve as point-like actuators, whereas linear ciliary bands and 2D ciliary carpets can produce a variety of hydrodynamical phenomena. We discuss how control of ensembles of cilia is facilitated by a mixture of mechanical, hydrodynamic, neural and chemical cues, which jointly produce emergent physical phenomena such as topological defects, metachronal waves and chaotic mixing. We argue that the collective behaviour of large ensembles of cilia is an outstanding problem, motivating the development of new ciliary physics grounded in active-matter theory.

Structure and dynamics of single cilia

Early observations of beating flagella, beginning in the 1930s, noted the similarity of their beating pattern to a travelling wave[12,13]. These ideas motivated models that framed ciliary beating as a hydrodynamics problem, with the dynamics parameterized by the slender-body force coefficients associated with the time-varying ciliary shape[7]. For example, longer cilia beat more slowly, suggesting that increased drag along the primary axis dampens an oscillatory driving force[1]. Lacking technologies enabling more detailed study of the molecular origin of beating, early researchers instead focused on the far-field dynamics, in which temporal variation may be neglected and each cilium produces a time-averaged steady velocity field. This motivated early study of fundamental force singularities in Stokes flow, forming the basis of the first fluid-dynamical models of locomotion by microorganisms[14,15]. Some early experimental work introduced the notion of a time-varying phase associated with ciliary beating, noting that swimming sperm cells or colonies of green algae display some ability to modulate their phase to produce collective motion[16,17]. However, the origin of this phase and its regulation remained unclear, and the diversity of different flagellar beat forms observed among unicellular algae led some early authors to conclude that ciliary-actuation mechanisms varied widely across different systems[13,18].

More recently, improvements in microscopy and image analysis have allowed quantitative measurements of ciliary dynamics to be combined with improved understanding of ciliary ultrastructure, leading to more precise measurement and explanation of the phase and periodicity of ciliary beating. In general, the motion of cilia arises from coupled chemical and mechanical processes occurring in the axoneme, a tube-shaped structure consisting of an arrangement of nine microtubule doublets (each ~25 nm in diameter) surrounding a central pair of microtubules (known as a 9 + 2 arrangement)[3,10] (FIG. 2). The outer microtubule doublets are mechanically coupled to one other via nexin links, and attached to each doublet are 'radial spokes', protein complexes that extend towards the central pair. The orientation of this inner doublet pair breaks the symmetry of the filament, defining the bending axis. The axoneme has finite bending rigidity and, under small applied shear, it deforms similarly to an elastic tube (with bending rigidity ~10^3 pN m^2)[19–22]. The relative cross-linkage of the inner doublet pair (and, thus, the overall stiffness of the axoneme) may be modulated by the cell[23].

Beating arises from the collective effects of dyneins, which are molecular motors that convert the chemical energy of ~10^5 adenosine triphosphate (ATP) molecules per beat into a relative sliding motion among the

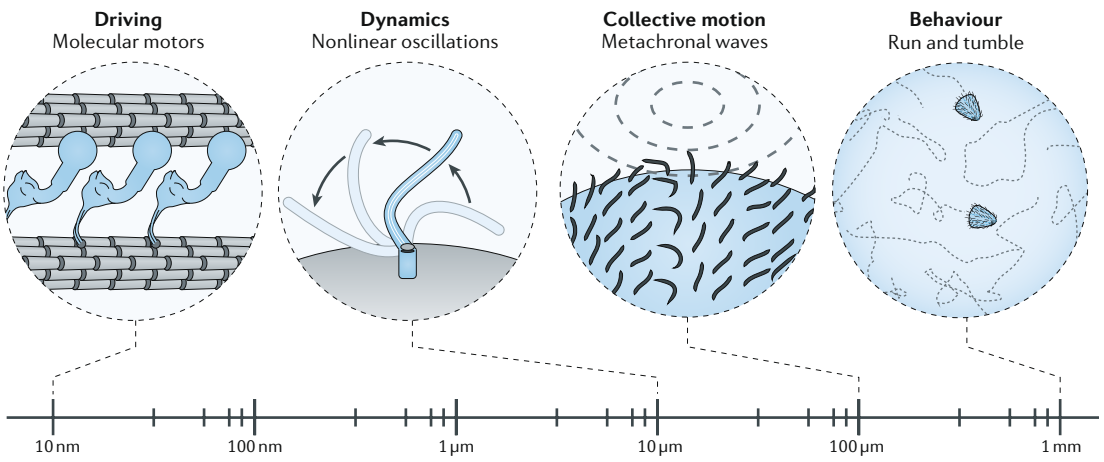

Fig. 1 | **Ciliary motion across scales.** On the scale of ~10 nm, cilia are driven by the motion of molecular motors on microtubule doublets. Cilia and their oscillations have a length scale of ~10 μm. Collective motion of ciliary sheets has a characteristic length scale of ~100 μm. The run-and-tumble motion of single-cell organisms, driven by cilia, occurs on a length scale of ~1 mm. Example length scales and timescales chosen to match those of the model protozoan *Tetrahymena*.

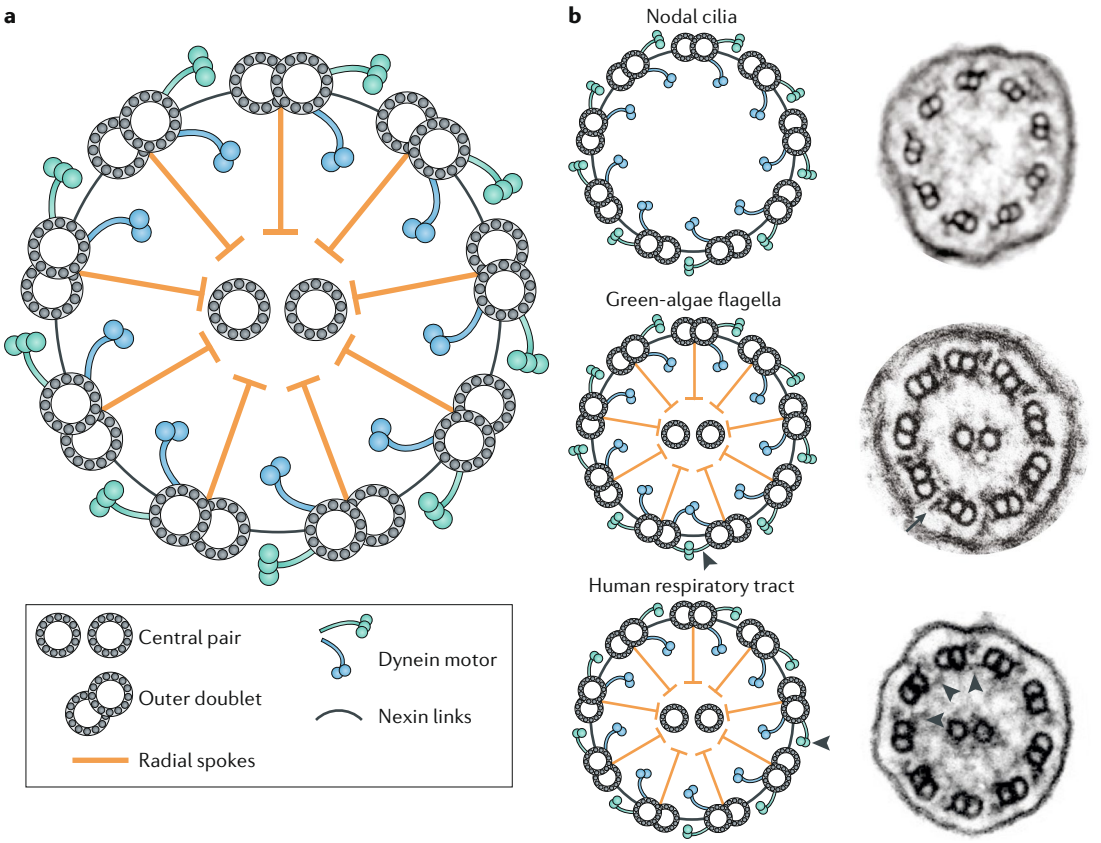

Fig. 2 | **Anatomy and structure of the axoneme. a** | A cross-sectional view of a typical axoneme, the structural scaffold of a cilium, showing the canonical '9 + 2' arrangement of microtubule doublets. **b** | Schematic views and transmission electron microscopy images of axoneme structures in specific ciliary systems: embryonic nodal cilia, the unicellular green algae *Chlamydomonas* and the human respiratory tract. The arrowheads indicate minor ultrastructural differences: a symmetry-breaking bridge in *Chlamydomonas* and the presence of only two outer dynein heads in human respiratory cilia[211–213]. Nodal cilium micrograph is reprinted with permission from REF.[214], Oxford University Press on behalf of the Japanese Society of Microscopy. Green-algae flagella micrograph is reprinted from REF.[215], with permission from Rockefeller University Press. Human respiratory tract micrograph is adapted with permission from REF.[216], Elsevier.

nine microtubule doublets comprising the axonemal sheath[10,24]. This motion causes a tension of ~10 nN to build up between neighbouring doublets[25]. There are several hypothesized mechanisms for how the sliding of dynein is regulated to produce beating. One possibility is the 'tug-of-war' model, in which dyneins antagonistically slide on opposite ends of the axoneme, causing longitudinal forces to continuously build up until dyneins on one side are forced to detach, breaking symmetry and causing the axoneme to bend[21,26]. Another proposed mechanism for regulation of dynein detachment is the 'geometric clutch' hypothesis[27], in which the bending of a 9 + 2 arrangement of microtubules under applied load modifies the interdoublet spacing of adjacent microtubules, which, in turn, causes dyneins to detach[28,29]. Notably, in the geometric clutch model, axonemal beating arises from negative feedback on dynein attachment, whereas in the tug-of-war model, positive feedback between opposing forces leads to beating as an instability.

However, experimental studies in sperm flagella have produced results inconsistent with both of these hypotheses for the regulation of dynein. Microtubules are seen to undergo differential sliding near the basal attachment point[30] and reconstruction of the distribution of applied forces (given the observed bending shapes) suggests that motor detachment is load-dependent[31]. More recently, direct imaging of individual substeps of the dynein cycle via electron cryotomography has shown that structures throughout the axoneme undergo conformational changes during the beat cycle, suggesting that control is distributed across a variety of asymmetric mechanical and chemical regulatory complexes[32].

A general regulatory mechanism that has gained recent experimental support posits a direct coupling between the local curvature of the axoneme and the attachment of dynein molecules[33]. In this model, the continuous transverse motion of dynein motors along filaments gradually increases the elastic stress in the system; this stress eventually stalls the motors and leads to reversal in their walking direction[34]. This process provides a dynamical closure for 'active filament' models, which model the coupled dynamics of dynein attachment and turnover, and the continuum mechanics of the axoneme[21,31,35]. Such models have a rich parameter space that captures many observed ciliary behaviours, including differential power strokes, multiple bending modes and stalling[36]. Variations of these models that include hydrodynamics can also reproduce both the

Box 1 | **Ciliary oscillations as active limit cycles**

Self-sustained beating requires three ingredients: the elasticity of sliding microtubule pairs, the viscous dynamics of the surrounding medium and the activity and regulation of molecular motors. From the combination of these elements, self-oscillation can emerge through a variety of mechanisms[11,26,27,34,66,191].

A natural starting point for modelling is the molecular motors themselves. At low order, each motor may be approximated as a two-state system[26,191]. Each motor is rigidly bound to a microtubule doublet 'backbone' and it then transiently binds and unbinds to a second, neighbouring microtubule doublet at a rate set by an effective potential U (see the figure). When bound, the motor generates a sliding force between the two microtubules by walking in a single direction. The binding potential U is superimposed on a harmonic potential describing the filament-bending dynamics, producing an overdamped dynamical equation

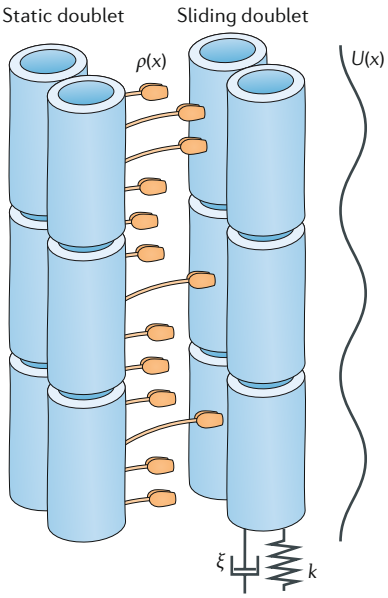

$$kX + \xi\dot{X} = -\int_0^L \rho(x)\frac{\partial}{\partial X}U(x-X)dx \quad (1)$$

where X is the filament position, $\rho(x)$ is the density of motors at position x along the backbone, L is the filament length, k is the elastic response parameter and ξ is the viscous response parameter. A schematic of this model is shown in the figure. The on and off rates of the motor are assumed to obey the uniform rate assumption $r_{on}+r_{off}=\Omega$, where Ω is a constant indicating the average transition rate[192].

A particularly elegant reduction of Eq. 1 occurs when $U=U_0(1-\cos(2\pi x/\ell))$, for which $r_{on}=\Omega(\eta-\alpha\cos(2\pi x/\ell))$[50,192]. Here, η is the fraction of the cycle in which the motor is active, U_0 sets the binding strength, α determines the degree of spatial variation in transition rates and ℓ is the filament structural periodicity. The following argument closely follows that of REFS[50,192]. The kinetic rates allow a chemical master equation to be defined for the system, which, under various assumptions[193], further reduces to a Fokker–Planck partial differential equation describing the joint distribution $P(X, \rho(x), t)$ of motor density $\rho(x)$ and filament positions. After applying a Fourier transform to $\rho(x)$, the dynamics of the first two modes a and b effectively decouple from the remaining modes, resulting in essentially a 2D dynamical system

$$\dot{a} = -\Omega\left(a + 1 - \gamma b^2 + 2\pi\nu bX/\ell\right),$$

$$\dot{b} = -\Omega\left((1+\gamma a)b + 2\pi\nu aX/\ell\right),$$

with the filament dynamics given by

$$\dot{X} = \frac{\Omega\ell}{2\pi}\left(\gamma b - \beta X/\ell\right), \quad (2)$$

where $\nu=k/(\xi\Omega)$ and $\gamma=2\pi^2\alpha U_0/(\Omega\ell^2\xi)$.

Ma et al.[50] show that, under appropriate change of variables, X can be mapped onto a single complex variable $Z=A\exp(i\theta)$, for which the dynamical system reduces to the Hopf normal form

$$\dot{Z} = \mu(\Lambda - |Z|^2)Z + i\left(\omega_c - \omega_1|Z|^2\right)Z \quad (3)$$

with $\mu=(3/2)\pi^2\Omega\nu(1+2\nu)/(1+4\nu)$, $\Lambda=(\Omega/2)(\gamma-\nu-1)/\mu$, $\omega_c=\Omega\sqrt{\nu}$, $\omega_1=-(\mu\sqrt{\nu})/(1+2\nu)$. Thus, an active filament subject to a cosine potential oscillates in a limit cycle with frequency $\omega_c-\omega_1\Lambda$.

These results demonstrate a minimal example of how sustained beating of a cilium or flagellum can arise naturally from a limit cycle in a minimal dynamical system describing the coupled dynamics of filament attachment, motor turnover and bending mechanics. These results are corroborated by experiments showing not only that unperturbed dynamics of flagella can be mapped onto corresponding limit cycles[50] but even that flagella under hydrodynamic load display behaviour consistent with forced oscillations[42].

corkscrew-like beating of isolated flagella and the planar beating of cilia, depending on the amplitude of the dynein activity term relative to the bending modulus[37]. We anticipate that further advancements in technologies allowing microscopic measurements of beating stages (particularly cryogenic electron microscopy) will help resolve ambiguities in the regulation of motor attachment, allowing further extension and refinement of these models[38].

One limitation of existing models is their emphasis on the ubiquitous, but not universal, 9 + 2 geometry of the axoneme. Notable exceptions to this layout are found in nature; in particular, nodal cilia found in developing embryos lack a central pair of microtubules and radial spokes. This causes these cilia to beat by sweeping a rotating arc, rather than a plane, resulting in chiral flows that serve to break the left–right symmetry of the developing embryo[39]. More exotic axoneme geometries can also occur, including so-called 9 + 9 + 2 microtubule arrangements, spirals and even patterns resembling Fibonacci sunflowers[40]. An open question remains whether such systems exhibit qualitatively different dynamical properties, caused by their unique geometry.

Regardless of the explicit geometry and chemo-mechanical dynamics, one generic view of cilia and flagella is as nonlinear oscillators executing a limit cycle[21,41]. Such a view allows models of swimming or collective behaviour to treat cilia abstractly as oscillatory forces driving the surrounding fluid (BOX 1). The phase and amplitude of these oscillations can be tuned through external driving. For example, experimental measurements of flagella under applied oscillatory flows confirm that flagella are capable of phase locking or stalling, depending on the amplitude or frequency of the driving flow[42–44]. Additionally, increasing the viscosity of the surrounding medium increases the spatial wavelength of beating while decreasing the beat frequency[7,13,45,46].

Owing to the finite number of dynein motors present within a given axoneme (~200 per μm)[27,47,48], ciliary and flagellar oscillations are also intrinsically noisy, exhibiting pronounced variation in beating rate, amplitude and timing precision, even within the same organism[49–51]. In the language of classical oscillator theory, the measured effective Q factor of flagella is 38.0 ± 16.7 (REF.[50]). Despite the noisiness of oscillations, the beat cycle is stabilized against changes in external conditions by the nonlinearity of dynein recruitment and detachment. For example, in detailed numerical simulations of 3D fluid–structure interactions on a beating cilium, details of dynein recruitment may be abstracted as an effective tension, the exact value of which has little effect on the presence of oscillations[52].

The role of nonlinearity in ensuring stable beating over a range of parameter values suggests that beating itself is a dynamical mode that can undergo bifurcation. Indeed, limit-cycle oscillator models of axonemes can undergo Hopf bifurcations between beating and quiescence, depending on both intrinsic parameters such as geometry and external cues such as viscosity or ATP availability[21,53]. These bifurcations are consistent with models of cilia based on explicit numerical models of the axoneme, which show that steady dynein forces and

fluid–structure interactions can jointly produce ciliary beating as a viscous 'flutter' instability[54–56]. One prediction of bifurcation theory is the dependence of stable oscillations on a minimum, critical ciliary length[21], an effect that has recently been directly observed in experiments in which the flagella of algal cells are grown to various lengths[57]. Generically, nonlinear bifurcations may confer axonemes with some degree of dynamical robustness, allowing them to respond to frequencies ranging from tens of Hz (typical beating rates for motile cilia) to several kHz (the frequency range of kinocilia in the human ear)[21].

Box 2 | **The dynamics of synchronization**

An oscillator that executes regular limit cycles can be transformed into an abstract 'phase' variable ϕ. If the oscillator's state variable x oscillates with natural frequency ω_0, then $\phi(t) \equiv \omega_0 \int_0^x \dot{x}^{-1} dx$. From experimental data, an instantaneous phase can be calculated via the Hilbert transform of x (REF. [67]). The phase maps the variable undergoing nonlinear oscillations — such as intracellular calcium concentration, cilium-tip displacement or axoneme deflection — to a new variable that increases linearly during the period of the oscillator. Working in phase coordinates simplifies theoretical analysis by scaling all external forces by how much they perturb a 'typical' cycle. This approach is always valid in the limit of small external forcing or coupling because, to leading order, perturbations affect the phase, but not the amplitude, of nonlinear oscillations[67]. Moreover, although phase oscillators are simplified models of cilia, their dynamical regimes match those observed both in experiments on flagellar ensembles and in 'rotor' models of cilia and flagella as rigid bodies revolving near a boundary[65,66,119,194].

In phase coordinates, two interacting oscillators with natural frequencies ω_1 and ω_2 have dynamics given by the Adler equation

$$\frac{d\Delta\phi}{dt} = \Delta\omega - \varepsilon \sin(\Delta\phi) + 2T_{\text{eff}}\xi(t), \quad (4)$$

where $\Delta\phi$ is the difference between the phases of the oscillators, ε is the coupling strength, $\Delta\omega \equiv \omega_1 - \omega_2$, T_{eff} is an effective temperature that sets the noise amplitude and the noise ξ obeys $\langle \xi(t)\xi(t') \rangle = \delta(t - t')$ when averaged over an ensemble of realizations. The parameters in Eq. 4 can be estimated from experimental data sets; REF. [72] describes a particularly elegant technique for fitting Eq. 4 to flagellar beating in green algae.

In the strong-coupling regime, $|\omega_1 - \omega_2| < \varepsilon$, hydrodynamic or mechanical coupling is stronger than the intrinsic difference between two oscillators. In this limit, a stable solution $\Delta\phi = 0$ is approached over timescales $\sim\varepsilon$; thus, phases lock faster under stronger coupling. The other limit $|\omega_1 - \omega_2| > \varepsilon$ corresponds to a drifting solution, in which the oscillators affect one another's phases without ever fully synchronizing. Depending on T_{eff}, noise can manifest as periodic 'slips' in the otherwise linear dynamics of the fully synchronized state; as $|\omega_1 - \omega_2| \to \varepsilon$, the dynamics becomes more sensitive to noise.

The Kuramoto model generalizes the coupling dynamics of the Adler equation to systems of many cilia, by formulating the dynamics of N non-identical phase oscillators in terms of the feedback of the weighted mean field on each individual

$$\dot{\theta}_i = \omega_i + \sum_{j=1}^{N} \frac{K_{ij}}{N} \sin(\theta_j - \theta_i). \quad (5)$$

Here, θ_i and ω_i are the phase and natural frequency of the ith oscillator and K_{ij} is the coupling between the ith and jth oscillators. The globally coupled case $K_{ij} = K$ is analytically tractable and displays several canonical behaviours observed in natural systems of coupled oscillators, including a transition between synchrony and disorder at a critical value of K (REF. [67]). However, non-global coupling, such as nearest-neighbour coupling, is more relevant to ciliary systems; under such conditions, Eq. 5 exhibits diverse behaviours, such as transient and localized synchronization. Certain classes of explicit hydrodynamic models of cilia can be reduced to dynamical equations of the form of Eq. 5 (REF. [92]); variations of these equations with alternative driving functions and coupling schemes reproduce phenomena seen in ciliary arrays, including travelling metachronal waves[65].

However, not all real-world ciliary systems have dynamics that can be fully captured by phase dynamics. Instead, models may be needed in which oscillators have both phase and amplitude dynamics, and nonlinear or time-structured interactions, such as pulse coupling[67,114]. The role of more complex and nonlinear couplings and interactions in flagellar synchronization has been explored through detailed continuum mechanical models and simulations[52,54,68,195]. Thus, beyond demonstrating established physical principles, such as Huygens synchronization, cilia arrays represent a potential test bed for new physics, with direct relevance to biology.

Ciliary synchronization

Ciliary coupling and synchronization. One of the first efforts to understand the collective behaviour of cilia dates to the first half of the 20th century, when scientists studying the swimming of bull sperm observed that two nearby sperm could locally entrain one another's tail beat, leading to synchronized swimming[58,59]. Later experiments established that, at high densities, this coupling can lead to collective flows[1], including large-scale vortex tilings that emerge when 8–12 sperm cells become mutually entrained[60]. Several recent studies have sought to better understand the origin of synchronization in small groups of flagella, with a goal of understanding how such dynamics affect the observed behaviours of flagellated microorganisms[61–63]. These experiments are motivated by a variety of theoretical models[13,64–66]. One particularly influential model developed by Andrej Vilfan and Frank Jülicher in 2006 models the hydrodynamic field of two cilia as a pair of spheres undergoing elliptical orbits near a boundary[66]. Depending on various spacing parameters, these model cilia exhibit a rich dynamical space that includes in-phase and antiphase synchronization, partial synchronization and other phenomena typically found in generic models of phase synchronization. We briefly review the physics of synchronization in BOX 2.

Experiments on somatic cells of the colonial alga *Volvox* have allowed the role of hydrodynamic coupling on flagellar beating to be readily identified. Each *Volvox* cell has two flagella that effectively act as one, and when pairs of cells are held at different separations using glass pipettes, the phases of the two flagella can be seen to couple over timescales inversely proportional to their separation[63]. This result directly confirms analytical models of cilia showing a direct analogy between hydrodynamic entrainment and phase synchronization[65,66]. This work demonstrates beautifully that two interacting flagella essentially represent a microscale version of classical Huygens synchronization, wherein the pendula of two neighbouring clocks are observed to gradually synchronize because of weak mechanical coupling[67].

In general, many classical topics in the physics of synchronization are relevant to understanding effects observed among groups of interacting cilia (BOX 2). However, the full dynamics of ciliary coupling are more complex than phase synchronization alone: detailed numerical simulations of beating filaments show that intriguing, higher-order effects can occur, including mechanical bistability[68] and load-dependent decoupling[69]. In biological contexts, these effects may lead to co-occurrence of in-phase and antiphase beating modes in multiflagellated cells, as well as a counterbend phenomenon in single flagella[22,70,71]. Additionally, mechanical buckling instabilities have been implicated in the steering mechanism of monoflagellated cells[53,54].

Hopf bifurcations
A Hopf bifurcation is a phenomenon occurring in many nonlinear dynamical systems, in which a periodic orbit spontaneously appears or disappears as a control parameter is varied.

Volvox
Commonly known as 'globe algae', these single-celled green algae form spherical colonies containing up to 50,000 cells.

Counterbend
A phenomenon in deforming elastic beams — and a deviation from classical Euler–Bernoulli beam theory — in which an applied curvature in one location induces a compensatory curvature elsewhere along the beam.

Run-and-tumble
A navigation strategy employed by bacteria and other microorganisms, in which an organism follows nutrient gradients by intermittently switching between directional swimming and random reorientation.

A system in which synchronization dynamics have clear biological relevance is the green alga *Chlamydomonas*, which uses two anterior flagella to pull itself through water in a manner reminiscent of breast stroke[72]. To increase photosynthetic yield, some strains of *Chlamydomonas* exhibit both positive and negative phototaxis, modulating their flagellar beating dynamics to approach or avoid light sources. High-speed imaging of *Chlamydomonas* cells held stationary by pipettes suggest that its two flagella indeed act like two coupled oscillators, displaying phase locking, synchronization and phase lag under forcing[73,74].

Order-of-magnitude calculations of synchronization timescales suggest that pairwise hydrodynamic interactions alone are an order of magnitude too weak to fully explain coupling and synchronization in *Chlamydomonas*[61]; thus multiple hypotheses exist regarding the coupling mechanism underlying flagellar synchronization. For example, experiments with freely swimming organisms suggest that negative feedback from torque generated during swimming may stabilize the synchronous state[75,76]. These results are consistent with Stokesian simulations, which suggest that time-varying drag due to the motion of the swimming body can affect synchronization[77]. However, recent studies using mutants of *Chlamydomonas* suggest that direct mechanical linkage via basal substructures likely explains the majority of synchronization dynamics observed under standard conditions[61,62]. Such structures present a compelling example of how the physical requirements of synchronization may have incentivized the evolution of specialized intracellular structures.

Ciliary coordination and microswimmer behaviour. Of particular relevance to the broader study of microswimmer physics is the onset and dynamics of synchronization among a small set of coupled cilia and flagella, a topic explored in several reviews[29,72,78,79,41]. In particular, synchronization dynamics and feedback-dependent modulation of ciliary and flagellar driving allows unicellular organisms lacking a nervous system to, nonetheless, execute a range of complex behaviours, moving beyond simple helical swimming towards gait switching and complex foraging strategies[79–81].

Experimental studies of the intersection between synchronization and behaviour have been performed in *Chlamydomonas*, in which transient coupling and uncoupling of a single flagellar pair produces either directed or disordered swimming, producing a eukaryotic analogue of classical run-and-tumble foraging[82]. That synchronization underlies this behaviour provides an elegant explanation for earlier studies that showed differences in helical swimming trajectories between algae with different flagellar beating dynamics[83], thereby providing a suggestive example of how synchronization dynamics enable behavioural complexity[1]. Accordingly, 'octoflagellate' green algae (which have eight flagella) display rich behavioural dynamics, such as repeated shocks and reversals that punctuate steady swimming[84]. Ciliated protozoans, including model systems such as *Paramecia* and *Tetrahymena*, have hundreds of cilia on their surface, providing them with sufficient degrees of freedom to display a large range of behaviours in response to external stimuli[85,86]. In *Tetrahymena*, specialized proteins have evolved that maintain mechanical linkage between the cilia and basal substructures under applied mechanical loads, stabilizing the swimming behaviour against changes in external conditions[87]. Furthermore, cilia can facilitate more complex behaviours than locomotion alone. For example, in the predatory protozoan *Lacrymaria olor*, spiral-shaped bundles of cilia surround a flexible 'neck', allowing the organism to actively track and hunt other microorganisms[88].

Ciliary coordination and multicellularity

An emerging focal point in ciliary biophysics involves unravelling the physics of coupled cilia in multicellular life. The emergence of complex multicellularity and early animals closely mirrors the evolution of new mechanisms of controlling cilia, and many striking examples of early cellular specialization are found in colonial flagellates and ciliates[89–91]. Intuitively, denser and more complex arrangements of cilia — such as chains or sheets on the surface of an organism — have a larger possible configuration space than isolated cilia, allowing them to exhibit both a wider range of physical phenomena and of biological functions that harness them. Indeed, theoretical studies that treat ciliary sheets as hydrodynamically coupled oscillators have reported striking collective phenomena ranging from spiral waves to topological defects in the spatial distribution of phases[92]. Here, we review experimental and theoretical studies of ciliary dynamics in multicellular systems and highlight the need for greater theoretical study of cilia in the 'large N' limit. We hope that such approaches may offer hints towards concepts unifying the diverse types of collective ciliary beating found in the animal kingdom.

A natural starting point is the choanoflagellates, colonial protozoans that represent the closest unicellular relative of modern animals[93]. Choanoflagellates consist of monoflagellated cells that can each swim individually, but which tend to aggregate into colonies that swim collectively. While these colonies swim more slowly than individual cells, the primary benefit of aggregation likely arises from cooperatively generated flows[94–97]. Such flows have the overall structure of a force dipole, increasing the feeding rate of the colony[97]. The beating dynamics of individual cells across a colony varies in time, an effect that has been hypothesized to allow the colony to chaotically mix the local fluid field over length scales larger than single cells[98]. However, although the distribution of flagellar orientations is nonrandom across a given colony, the individual cells in a colony are not spaced sufficiently closely to hydrodynamically entrain one another[97] and, thus, the overall motion of the colony has the statistics of a random walk aggregated among several independent actuators[99]. Additionally, long-term analysis of the statistics of colony motion suggests that these collective flows can be modulated over time via hydrodynamic signalling, allowing clusters of cells to implement long-term search strategies analogous to run-and-tumble locomotion[100]. As close ancestors of modern animals, choanoflagellates thus represent a context in which the synchronization dynamics and hydrodynamics of cilia collectively give

rise to flexible behavioural strategies, providing a preview of how collective physical effects incentivized the development of multicellularity.

In the first true animals, cilia appeared in specialized cell types lining epithelial surfaces[3,7]. In these cases, cilia serve the same basic function that they serve in unicellular life: facilitating locomotion and basic sensing. For example, sponges use ciliated tissues to drive large-scale flows through intricate internal canal systems, allowing them to filter their own volume in water in less than a minute[101,102]. The ciliated cells lining the body cavities of sponges are termed choanocytes due to their unique 'collared' shape, which has strong physical resemblance to choanoflagellates (although the exact evolutionary relationship between the two cell types is debated)[103,104]. The characteristic radii and number of channels found in sponge vasculature follows predicted scaling laws for optimal transport in laminar flows[105] and the placement of pumping choanocyte chambers allows load-balancing across the network[106]. Thus, sponges represent a system in which hydrodynamic transport considerations strongly influence the geometry and placement of ciliated cells relative to other cell types. Similar considerations may exist in systems beyond sponges. Corals are another basal, colonial animal that leverage ciliary flows, creating beautiful arrays of counterrotating vortices that enhance surface nutrient and oxygen transport[107].

In later-diverging basal invertebrates, coordination of cilia enables more complex locomotion and behaviour. The amoeboid-like animal Placozoa comprises a quasi-2D sheet of ciliated cells, which collectively organize their beating directions to produce coordinated locomotion and large-scale tissue deformations[108,109]. These cells coordinate without the aid of a nervous system; recent work has found that they use elastomechanical coupling via intercellular junctions to create a ciliary analogue of flocking[108–110]. In this system, collective ciliary motion can generate a range of complex behaviours, ranging from rotational and translational motion (akin to run-and-tumble motion) to rhythmic 'freezes' (ciliary frustration) lasting 5×10^5 ciliary beats, during which the animal flattens and feeds[110,111]. However, recently, it has become evident that a complex collection of neuropeptides can also regulate ciliary dynamics (and, thus, behaviour) over longer timescales, suggesting that the mechanical and hydrodynamic mechanisms that govern locomotion over short timescales are themselves modulated by signalling pathways over longer periods[112].

Among extant animals, cilia with nearly identical ultrastructural features are found organized in a variety of geometries and densities, ranging from point-like 'tufts' that sense fluid shear, to curved bands that generate feeding currents, to dense carpets that pump bodily fluids[7,14,113] (FIG. 3). This diversity of geometries is matched by a diversity of functions, ranging from shear sensing, to nutrient filtration, to locomotion (FIG. 4). This diversity motivates extending existing theoretical approaches. For example, how does non-uniform substrate curvature affect hydrodynamic interactions between cilia and, therefore, synchronization? Can such effects be captured by existing hydrodynamic oscillator models, or do new phenomena arise that require modelling of details that are not needed in models of smaller systems? Some indication of the possible dynamical richness of cilia in multicellular systems can be inferred from recent developments in oscillator physics (BOX 3), which have shown that models with features such as intermediate-range coupling, nonlinear forcing and pulse coupling can lead to exotic dynamics such as glassy states and partial synchronization[114,115].

The possible role of physical arguments for understanding the diversity of cilia found in animal systems can be seen by considering beating frequency versus ciliary length — two dynamical parameters that describe cilia on a microscopic scale — or generated flow speed versus interciliary spacing — two dynamical parameters that characterize macroscopic ciliary ensembles (FIG. 5). The data suggest an inverse relationship between the parameters — scalings that are intuitive from an energetic standpoint[14,94] — although the trend in flow speed versus spacing is weaker, likely due to different developmental mechanisms and higher-order hydrodynamic effects present in high-density ciliary systems. We caution against drawing conclusions from the data plotted in FIG. 5 alone, which sampled systems primarily based on the availability of these four parameters in existing studies. Nonetheless, these data suggest that, although cilia across the animal kingdom are heterogeneous in their dynamical parameters, their operating range and efficiency is, nonetheless, constrained by basic physical limitations.

Beyond diversity in arrangement, cilia in multicellular life are also characterized by a large-scale control mechanism in the form of the nervous system[116–118]. Neurociliary coupling allows local interactions between cilia via hydrodynamic and elastic couplings to be complemented by global signals based on the organism's

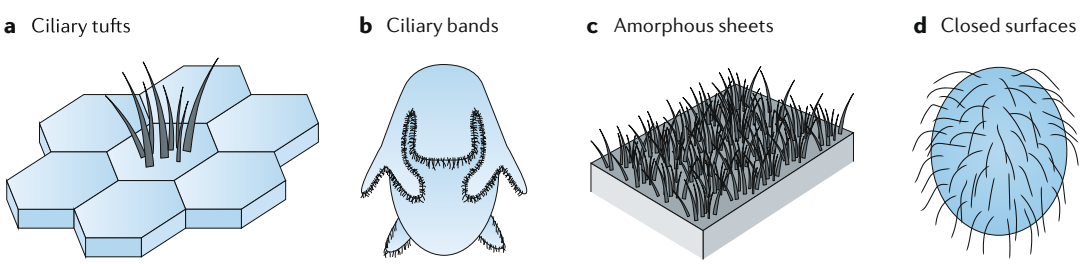

Fig. 3 | **Ciliary geometries in animal systems.** The diverse range of ciliary geometries found in animal systems includes point-like ciliary tufts (zero dimensions; part **a**), linear ciliary bands (one dimension; part **b**), amorphous sheets (two dimensions; part **c**) and closed surfaces covered with cilia (two dimensions with curvature; part **d**).

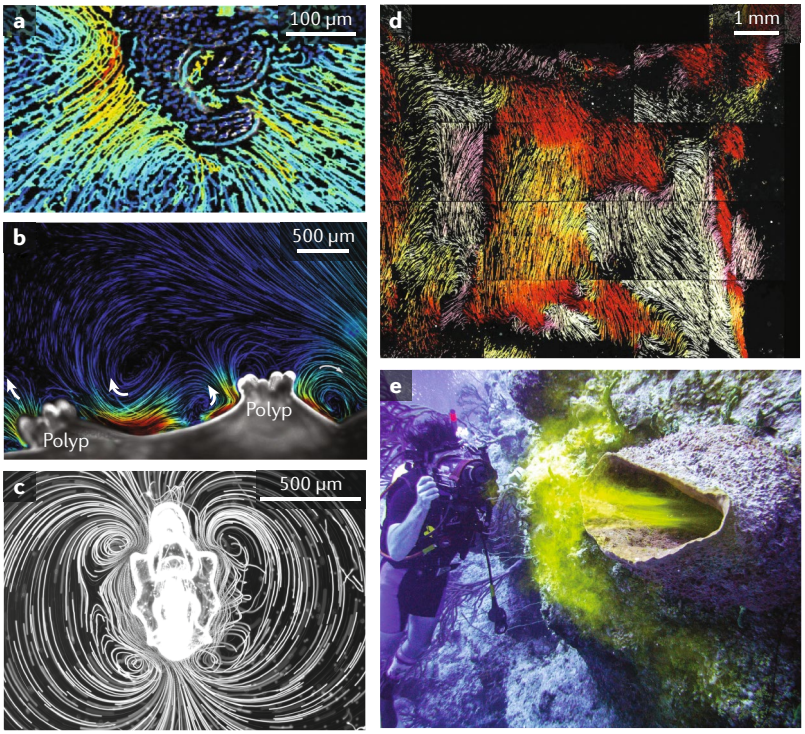

Fig. 4 | **Ciliary hydrodynamics in animal systems. a** | Particle-filtering flows used for microbiome recruitment by the Hawaiian bobtail squid. The hue indicates relative speed. **b** | Vortical flows used by coral reefs to enhance nutrient and oxygen uptake. **c** | Feeding and swimming currents created by a starfish larva. **d** | Coordinated flows created by the ciliated epithelium of a pig-brain ventricle. **e** | Large-scale feeding flows created by a reef sponge. Panel **a** is reprinted with permission from REF.[184], PNAS. Panel **b** is adapted with permission from REF.[107], PNAS. Panel **d** is adapted with permission from REF.[146], AAAS. Image in panel **e** courtesy of Steven E. McMurray, University of North Carolina Wilmington, USA.

sensory inputs. There is a relative scarcity of theoretical studies that directly augment canonical models of interacting cilia (such as coupled oscillators or hydrodynamic rotors) with global modulation via an external field (such as a fixed, time-varying 'control' phase added to each cilium's phase). However, we note that the timescale of neuronal dynamics (~1 ms) is often well separated from reported timescales of ciliary synchronization (~100 ms), suggesting that, as a starting point, the nervous system may be abstracted as an intermittent, rapid perturbation to existing dynamical modes that arise primarily from the synchronization dynamics. For more detailed models, we anticipate that insights may be found in the field of active-matter physics, which has sought to relate mechanistic insight into individuals (such as particle or agent models) to collective effects (such as collective motion or flocking).

We thus hypothesize that an emerging frontier in ciliary physics will involve bridging experiments and theory in a few ciliary systems with the complexity of geometries and control mechanisms available in animal systems. Below, we highlight two existing areas of particular relevance to bridging the physics of cilia across the microscopic and macroscopic scales in animal systems: collective pumping generated by 2D ciliary sheets, and feeding currents created by the 1D ciliary bands of invertebrate larvae.

Reynolds numbers
Dimensionless quantity expressing the ratio of inertial to viscous forces in a fluid dynamics problem. Navigation and locomotion strategies are qualitatively different in the low-Reynolds-number (overdamped) regime and high-Reynolds-number (turbulent) regime.

Collective flows in ciliary sheets. Historically, a multicellular context in which cilia have received particular attention is ciliary sheets, which appear in diverse contexts ranging from the gill filters of molluscs, to the lining of the mammalian trachea, to the ventricles of the brain[7]. As a first approximation, such sheets can be considered a high-density limit of the 'coupled oscillator' models described above[65,119,120]. Adjacent cilia entrain one another, leading portions of the ciliary sheet to beat in phase. However, over larger distances, non-adjacent cilia can couple together through the collective flows generated by the array, leading to mesoscale phenomena not seen in few-cilia or flagellar systems. For this reason, ciliary sheets have been the focus of recent efforts to observe complex synchronization phenomena that require more intricate interactions than those found in traditional phase oscillator models (see BOX 3 for several examples).

A well-studied emergent phenomenon in ciliary sheets is metachronal waves (named from the Greek for 'time after'), corresponding to groups of cilia that beat in succession, giving rise to propagating waves that travel across the array. Cilia on the edge of each travelling wave have the same phase; in the case of evenly spaced rows of cilia, closely spaced cilia within a row hydrodynamically synchronize and beat in phase, whereas different rows have phase lags relative to one another as the metachronal wave passes[14,121]. The resulting smooth, progressive motion of cilia across the array resembles the motion of corn stalks in a windy field[7].

Four types of metachronal waves have been reported, which correspond to the four allowed chiralities of waves relative to the ciliary beat plane: a pair of longitudinal waves that travel either along or against each cilium's individual beating direction (corresponding to a positive or negative phase lag between successive cilia) and right-handed and left-handed transverse waves in which the cilia predominantly beat out-of-plane relative to the propagation direction[122]. Consistent with theory, forward-travelling longitudinal — also known as symplectic — waves have lower speed but larger torque; in biological contexts, these waves often function to transport large particles or mucous[123]. The other three wave classes travel faster and usually produce large-scale water currents or swimming strokes[7]. Numerical models of hydrodynamically coupled ciliary arrays have shown that nearly symplectic metachronal waves naturally arise in such systems[69,124], demonstrating that global synchronization is not inevitable in ciliary arrays, despite the long range of hydrodynamic coupling forces at low Reynolds numbers.

A major function of metachronal waves, and ciliary arrays in general, is to collectively pump fluids at low Reynolds numbers — for cellular locomotion, or for transporting mucous and other bodily fluids. For this reason, artificial ciliary arrays using magnetically actuated filaments is an area of active research, particularly for implementing pumping and mixing in microfluidic devices[125–127]. For a given system, the parameters of the travelling metachronal waves, such as the speed and spatial scale, dictates their function in different contexts. Experimental studies in protozoa and in animal mucous membranes have shown that increasing local

viscosity decreases the beating frequency of individual cilia, which either increases or decreases the speed of metachronal waves, depending on whether the waves are symplectic or not[18,45,46,128]. This phenomenon represents a mismatch between the phase velocity (associated with individual beating rates) and the group velocity (associated with travelling waves), illustrating the importance of wave properties in characterizing a given metachronal wave system. Importantly, shorter-wavelength metachronal waves apply less force locally but transport fluid faster, because each front has fewer cilia driving it[7]. Such observations are consistent with more detailed theoretical models showing a physical trade-off between applied forcing and maximum transport speed in ciliary arrays[64,129,130]. Ciliary sheets that exhibit metachronal waves have pumping speeds that vary over three orders of magnitude across different organisms, a trend that is potentially related to variation in ciliary density (FIG. 5b).

Reconstruction of beating patterns observed in experimental data sets underscores that pumping rate alone does not dictate the phenomenology of metachronal waves. Numerical simulations reveal that experimentally observed metachronal waves qualitatively match optimal waveforms for efficient pumping[131]; however, in some systems, the exact distribution of phase differences seen in experimental data may, nonetheless, differ substantially from the predicted global optimum[132,133]. Possible constraints leading to suboptimal pumping rates include limitations on the availability of ATP or dynein molecules within the axoneme of each cilium[134], heterogeneous fluid viscoelasticity in the ciliary sublayer[135,136] and higher-order damping modes incompletely captured in numerical models[127].

However, another explanation for these findings is that selection forces on metachronal waves do not seek to maximize the pumping speed outright; rather, they seek to minimize the total energy dissipation, given a target pumping speed. Indeed, computational studies indicate that, when compared with global synchronization, metachronal waves increase pumping speeds by only a factor of 3, but they increase pumping efficiency by a factor of nearly 10 (REF.[124]). Direct measurements of ATP consumption in demembranated sperm flagella using a fluorescent reporter[24] and pH probes[137] estimate that isolated flagella consume ATP at a rate of ~10^5 molecules per cycle; these consumption rates are observed to scale linearly with beating frequency and inversely with the viscosity of the surrounding fluid. Because partial synchronization reduces the effective drag on a cilium[41,138] (in both ciliary arrays and isolated flagellar pairs), it follows that cells may dynamically decrease ATP consumption through metachronal waves or synchronized beating. However, several computational studies suggest that ciliary beating, even in collective settings, still exhibits suboptimal energetic efficiency[132,133]. We speculate that this suboptimality arises because, beyond purely biophysical constraints, evolutionary history also plays a role in establishing the form of metachronal waves. For example, experimental studies have shown that related families of molluscs, despite having nearly identical ciliated gills, can exhibit markedly different metachronal waves[122].

Beyond metachronal waves, ciliary sheets display a variety of other hydrodynamic phenomena. Numerical studies of 2D planar carpets of beating cilia report two distinct fluid-dynamical regimes: above the ciliary tips, smooth laminar flow dominates; however, below the ciliary tips, the flow becomes chaotic, with entrained tracer particles hopping irregularly from cilium to cilium, tracing scribbled trajectories[139]. Explicit 'sublayer' models of cilia-driven flows provide some intuition for how such chaotic dynamics naturally arise from even minor stochasticity in beating phase or phase misalignments

Box 3 | Frontiers in synchronization and experimental analogues of ciliary arrays

Phase oscillator models with different assumptions to that of the 'standard' Kuramoto model reveal new phenomena, with direct relevance to complex ciliary dynamics in multicellular organisms. One particularly relevant set of systems are Kuramoto models with inhomogeneous coupling. In ciliary and other oscillatory systems, coupling is not necessarily uniform and all-to-all, but may instead be localized — either by finite-range hydrodynamic effects (such as inertial screening) or by short-range mechanical interaction through basal substructures[61,62,196]. Arrays of oscillators with non-uniform interactions display unique phenomena, such as the emergence of phase slips in propagating waves, spontaneous desynchronization transitions and glass-like relaxation[197–201].

A phenomenon of particular interest is chimaera states, which occur when synchronized and desynchronous subpopulations coexist in an ensemble of oscillators[181,182]. A minimal example of a chimaera consists of two coupled oscillator populations with stronger intrapopulation coupling than interpopulation coupling[202]. For cilia, these two oscillator populations might represent non-contiguous ciliary tufts at different locations on an organism or cilia residing in areas of high or low body curvature[115,180]. This model displays low-dimensional dynamics parameterized by the order parameters of the two subpopulations, including a bifurcation from a stable chimaera to a slowly-evolving 'breather' state[202]. Similar two-population chimaera states occur in more biologically relevant (although less mathematically tractable) models, such as discrete oscillator models with next-nearest-neighbour interaction, and continuum models with coupling amplitude that decays slowly with spatial radius[115,181,182]. Chimera states are a particularly intriguing phenomenon to seek in ciliary systems[155,156,203] because they represent a mechanism by which a ciliary array can simultaneously exhibit multiple, large-scale beating patterns, even in the absence of explicit large-scale control (such as a central nervous system)[204].

Although chimeras, glassy states and other recently discovered phenomena from synchronization theory have yet to be directly observed in living cilia, many of these phenomena have been observed in synthetic analogues of cilia. One such system consists of micrometre-scale colloidal particles held in optical traps, which serve to drive the particles along predetermined trajectories[176]. Multiple particles (in separate traps) interact hydrodynamically, and when proximal particles are driven along concentric circular paths tangential to a nearby wall, the system is a physical realization of well-studied rotor models of ciliary chains and sheets[65,66,119,183,194,205]. These colloidal rotors match the spatiotemporal dynamics of true flagellar flow fields down to their characteristic length scale of ~10 μm[156]. These synthetic cilia exhibit many non-trivial behaviours associated with nonlinear oscillators, including long-lived phase defects, nonlinear synchronization profiles (such as Arnold tongues) and transient epochs of partial desynchronization reminiscent of true chimaera states[156,176].

Other experimental analogues of cilia may allow large-scale investigation of problems at the intersection of ciliary biophysics and synchronization theory. One such system consists of driven magnetic microparticles, which can be assembled into rods and chains to create active filaments[125,127,206]. These systems allow large numbers of interacting filaments to be studied at scale, potentially allowing the observation of large-scale collective effects such as phase domains and spiral waves[92]. Similar effects are possible in experiments in which single flagellated cells are adhered to a surface, forming synthetic ciliary sheets with controllable densities[152,153,207,208]. At smaller length scales, in vitro experiments with microtubule bundles driven by kinesin motors have successfully produced metachronal waves and dynamic nematic domains[209,210], suggesting the potential for such systems to capture how orientational defects in the ciliary field affect synchronization.

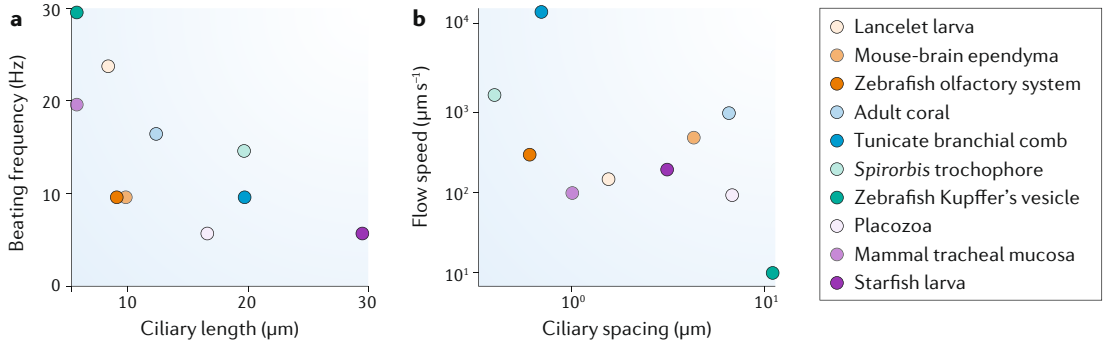

Fig. 5 | **Ciliary parameters across animal systems. a** | Trends in microscopic parameters, namely beating rate versus ciliary length. **b** | Trends in macroscopic properties, namely flow speed versus ciliary spacing. For cases in which a range is reported, we plot the mean. Data taken from REFS[7,14,39,107,108,123,146,186,217–222].

between adjacent cilia[1,140,141,144]. Experimental studies of magnetically driven artificial cilia confirm these distinct regimes[126,139,142], which allow simultaneous pumping or swimming in the far field, while allowing mixing and reoxygenation of fluid near individual cells. These results are consistent with particle-tracking experiments performed in ciliated vesicles of zebrafish embryos[143].

The large-scale fluid-dynamical fields created by ciliary sheets also display interesting physical phenomena. The trachea and other mucous membranes of many animals contain ciliary sheets that pump mucous, helping to filter contaminants out of the airway[144,145]. The multiciliated cells of these mucous membranes are arranged in an intricate patchwork pattern with orientational noise embedded in individual ciliary beat directions, resulting in distinct local flow regimes determined by the neighbour topology of the epithelium[144]. Additionally, recent work has shown that ciliated surfaces in the brain, which transport cerebrospinal fluid, implement precise fluidic motions, depending on an animal's resting state and other global neurological cues[146–148]. Intriguingly, these cilia have recently been shown to synchronize their beating via purely hydrodynamic coupling mechanisms[148]. Such observations demonstrate how ciliary sheets leverage the many degrees of freedom intrinsic to ciliary arrays, in order to precisely control physiological flows.

One parameter of large-scale ciliary arrays that appears to be strongly developmentally regulated is the relative orientation of cilia comprising the array. The ependymal ciliary beating plane arises from planar cell-polarization mechanisms, a series of genetically encoded developmental pathways that also dictate the position of nodal cilia, which serve to break left–right symmetry in developing embryos[149,150]. The origin of beating-plane orientation and chirality in the beat forms of individual cilia is less well understood, but theoretical models indicate that the two chiralities are dynamically bistable, suggesting that beating chirality could, in principle, be controlled by exogenous factors, rather than developmental patterning[151].

These observations and models motivate the development of models of ciliary sheets that can account for topological effects among large numbers of cilia. The recently developed theoretical framework of 'active-carpet' models — originally developed to understand transport in biofilms — has illustrated how features such as gradients in the local director field associated with ciliary beating can give rise to strongly localized flows[152,153]. These flows can produce uniform vortex arrays or chaotic streamlines, depending on the relative placement of topological defects, thereby coupling local features with the global properties of the flow field. Topological features can also arise in the relative phases of cilia in an array, an effect observed in 'rotor' models of cilia (which are analogous to classical phase oscillator models)[92,154,155]. Dynamical behaviours ranging from coarsening defects to spiral waves can emerge in these models; their appearance is controlled by a parameter that specifies the direction of torque on each rotor — a term mathematically similar to introducing a phase delay into the Kuramoto model of phase oscillators (BOX 2), which exhibits similar dynamical phenomena[92].

We anticipate that future studies will use models that draw an explicit analogy between ciliary beating and classical spin models: each cilium has a location and a beating direction, and it interacts both with its nearest neighbours through direct coupling and with the mean field through hydrodynamic shear. Thus, it is intuitive to expect ciliary arrays to support many phenomena seen in classical spin systems, such as frustration, defects and grain boundaries[41].

However, standard spin models are equilibrium systems; by contrast, ciliary oscillations are intrinsically a non-equilibrium phenomenon. For this reason, phase and oscillator-based models, which are driven, provide a natural starting point when extending classical spin theories to model cilia. Indeed, oscillator models have successfully demonstrated a variety of effects unique to ciliary systems, such as metachronal waves and switching between alternative beating modes, which propagate similarly to solitons[65,124,156]. Such analogies lead to the interesting question of whether known features of 'active' spin models can occur in ciliary sheets, such as flocking effects, finite size scaling and unusual temperature-dependent phases (with the intrinsic noise of individual ciliary beat cycles setting the effective temperature)[50,155,157]. Further motivation for revisiting such models comes from experimental observations of topological effects, including orientational defects and grain boundaries, in a variety of ciliary systems[146,158–161].

Ependymal
Referring to a thin membrane of cells lining the ventricles of the brain and the central canal of the spinal cord. These cells play a central role in supporting neuronal function.

Coarsening
A phenomenon in the dynamics of spatially varying scalar fields, in which small-wavelength features are gradually consolidated into larger-wavelength patterns.

Solitons
Travelling, bounded wave packets occurring in nonlinear media that propagate at fixed velocity.

Ciliary bands and the evolution of the nervous system. Cilia also played a crucial role in diversification of animal body plans. The first animals were marine invertebrates, which developed a diverse range of body morphologies and life-history strategies in response to the vicissitudes of the oceanic environment. Among these adaptations is indirect development: rather than proceeding directly from an embryo to the adult body plan, many invertebrates pass through freely swimming, microscopic larval stages with distinct appearances from their adult form[162]. The alien appearance of these microscopic larvae, as well as their ubiquity among invertebrates, captivated 19th-century biologists, who saw them as a starting point for deciphering the animal tree of life[90,163].

From a physicist's perspective, invertebrate larvae are particularly intriguing because they swim at low Reynolds number, implying strong viscous constraints on the strategies and morphologies available for locomotion. Almost all invertebrate larvae swim and feed using ciliary bands: dense, linear arrangements of cilia that encircle the larva's body and that are controlled by the larval nervous system. In ciliary bands, hundreds of thousands of cilia are packed together so densely that 19th-century zoologists termed them 'vibratile chords', in reference to their shimmering appearance under low magnification[164]. These bands have a typical length 100 µm–1 mm and ciliary spacings as small as 100 nm, suggesting that hydrodynamical and other physical interactions strongly determine collective effects in these systems[163]. Existing quantitative models have categorized the large-scale hydrodynamic properties of ciliary bands, such as their swimming efficiency or hydrodynamic capture cross section in feeding larvae[113,165,166]. Certain ciliary-band geometries — such as those with an inverted, helical shape — give rise to qualitatively different structures in the local flow field around the larvae, creating geometrically distinct trapping regions and, thus, feeding efficiencies[166]. The exact mechanism of filter feeding depends on the animal: some larvae use cilia to directly intercept passing particles, whereas others use strong hydrodynamic shear forces to funnel particles towards their mouths[166–168]. Additionally, the types of beating patterns collectively produced by the cilia likely influence the efficiency of each capture strategy[169]. Due to their diverse, neuronally controlled functions across many invertebrates, it has been hypothesized that the need to control ciliary bands formed the impetus for the evolution of the first animal nervous systems[162].

At larger scales, flows produced by ciliary bands display hydrodynamic phenomena not typically observed at low Reynolds numbers. High-speed imaging of starfish larvae, a model system for invertebrate development, reveals ciliary flows consisting of dozens of counter-rotating vortices around the animal's periphery. These vortices coalesce and reform over time as the animal gradually modulates its ciliary beating[158,170]. Because power dissipation at low Reynolds numbers is proportional to the squared vorticity, these structures require continuous energy investment on the part of the organism, a cost potentially offset by the adaptive advantage of these vortex fields for capturing prey. Additionally, neural modulation of ciliary beating produces unexpected effects such as Lagrangian chaos in the local flow field, further enhancing feeding rates[171]. Such phenomena likely appear in a range of invertebrate systems with ciliary bands[172]; however, experimentally cataloguing these systems will require the development of improved microscopy tools for probing ciliary beating and fluid dynamics at planktonic scales (~10 µm–10 mm), such as 3D tracking microscopy[173–175].

The complexity of the flow fields around ciliary bands arises from complexity in the underlying ciliary-beat patterns. Micrographs of cilia on the band reveal point-like topological defects, where cilia either bundle together or splay apart due to discontinuities in the boundary conditions induced by nearby stagnation points[158,171]. Both experimental and theoretical models of coupled hydrodynamic rotors (which have comparable dynamics to phase oscillators) suggest that topological defects can arise spontaneously due to intermediate-scale ciliary coupling, suggesting that the defects potentially arise from nonlinearities in coupling[156,176]. However, it is likely that the locations of defects are determined, at least in part, by external cues — either by anatomical patterns in substrate rigidity or via input from the nervous system. Nonetheless, rotor models indicate that topological defects likely have implications for the types of metachronal waves and other beating patterns possible in their vicinity.

Ciliary bands exhibit a rich morphospace, and surveys of invertebrates have catalogued a variety of surprising and intricate ciliary-band geometries[113]. The structure of these bands and the emergence of topological features likely have direct biological implications. For example, during the development of the sea lily *Metacrinus*, the ciliary bands change topology over a period of several weeks, switching shape from a single, winding contour to a series of small, interconnected curves outlining the surface of the animal[177]. Presumably, this topological transition produces a qualitative change in the local hydrodynamics, affecting the feeding and swimming strategies of the animal.

From the perspective of oscillator models of cilia, a particularly relevant line of theoretical work for understanding band diversity is curvature-mediated synchronization[115]. Hydrodynamic rotor models of cilia on the surface of a sphere show that metachronal waves and other dynamic instabilities can arise due to local curvature or inhomogenous ciliary density, which amplify the effect of small-scale heterogeneity among cilia[178,179]. This provides a minimal example of how geometry and dynamics may be coupled in ciliary bands. Complementary theoretical work on coupled oscillator arrays has demonstrated that curvature can produce localized subregions of synchronized oscillators[180], even while the remainder of the arrays remains desynchronized. Such localization represents the 'spot' form of chimaera states, a recently discovered phenomenon in phase oscillators[181,182] (see BOX 3 for a description of chimeras). Ciliary bands tracing complex contours on a larval surface can, therefore, exhibit differential synchronization and metachrony based on local anatomy, potentially explaining differences in hydrodynamic fields observed in different regions around larvae[113,165,166].

Lagrangian chaos
Chaotic motion of tracer particles in a fluid, which readily occurs in high-Reynolds-number flows (such as turbulence). Under certain conditions, it can also occur in the low-Reynolds-number flows produced by ciliated microorganisms.

Morphospace
An abstract coordinate system describing all possible forms or shapes of an organism, parameterized by a small number of independent variables.

Due to their intricate topologies, nervous control and central role in animal evolution, ciliary bands thus constitute a potential focal point for future work understanding emergent physics in ciliary arrays. That ciliary bands essentially represent a 1D, dense array of cilia — albeit one embedded on a complex 3D morphology — suggests that they offer a new context for testing classic 1D models of collective phenomena in ciliary chains[65,183]. Intriguingly, ciliary bands are also subject to central nervous control by the organism, which may play the role of an external field that facilitates nonlocal synchronization across the band. Experiments in driven arrays of colloidal particles offer a glimpse of the dynamical richness of ciliary bands modulated by a long-range signal, demonstrating that, as long-range coupling increases, metachronal waves give way to incomplete synchronization punctuated by phase slips[156].

Emerging directions

The examples that we highlight in the previous section represent only a fraction of the diverse specializations and functions of cilia in the animal kingdom. Recent years have produced examples of diverse ciliary-driven processes, such as active microbiome recruitment by Hawaiian bobtail squids[184], a treadmilling-to-flapping transition in mollusc swimming[185] and mixing flows that enhance olfactory sensitivity in zebrafish[186]. In these systems, flow control and sensing are tightly linked, underscoring the need for new theoretical frameworks borrowing concepts from domains beyond active matter and fluid physics. One potential source of inspiration is 'embodiment', a conceptual framework developed in the past few decades that seeks to identify cases in which computation is performed at the level of the local physical response of an appendage, rather than by centralized nervous control[187,188]. In both robotic and living systems, embodiment quantifies the degree to which an organism can avoid neural centralization and its associated cognitive or developmental costs by instead performing 'morphological computation'; for example, by having a compliant joint that mechanically adapts to a variety of applied loads[189].

Given the strong hydrodynamic coupling and collective dynamics of ciliary sheets, a natural, broad question for such research is how ciliary dynamics fit within the broader embodiment literature and how such theories can help explain the evolution of nervous control in animal systems[190]. Embodiment arguments may give insight into the neural requirements necessary to sustain a given degree of coherence in a ciliary array, by relating the sparsity of sensing apparatuses and neural loci to the observed beating dynamics. Recently, connectomics techniques have made it possible to explicitly map the whole-body neuronal circuits that control and distribute ciliary coordination in the larvae of the marine annelid *Platynereis dumerilii*[118], providing insights into how decentralized neural circuits can consolidate sensory information and induce large-scale behavioural changes (such as startle responses) in a basal metazoan[117]. These insights motivate us to speculate whether these neurobiological observations may be reconciled with physical models for control in spatially extended ciliary systems. Additionally, a major success of the embodiment literature has been the translation of organismal insights into bio-inspired technologies, especially in robotics[187,189]. Analogously, we hypothesize that understanding the limits of control in natural ciliary arrays will improve the responsiveness and sensitivity of cilia-inspired microfluidic pumps and filters[125–127].

Published online: 03 January 2020

1. Brennen, C. & Winet, H. Fluid mechanics of propulsion by cilia and flagella. *Annu. Rev. Fluid Mech.* **9**, 339–398 (1977).
2. Satir, P., Mitchell, D. R. & Jékely, G. How did the cilium evolve? *Curr. Top. Dev. Biol.* **85**, 63–82 (2008).
3. Marshall, W. F. & Nonaka, S. Cilia: tuning in to the cell's antenna. *Curr. Biol.* **16**, R604–R614 (2006).
4. Shah, A. S., Ben-Shahar, Y., Moninger, T. O., Kline, J. N. & Welsh, M. J. Motile cilia of human airway epithelia are chemosensory. *Science* **325**, 1131–1134 (2009).
5. Goetz, J. G. et al. Endothelial cilia mediate low flow sensing during zebrafish vascular development. *Cell Rep.* **6**, 799–808 (2014).
6. Clapham, D. E. TRP channels as cellular sensors. *Nature* **426**, 517–524 (2003).
7. Sleigh, M. A. *The Biology of Cilia and Flagella* (Pergamon, 1962).
8. Wan, K. Y. Coordination of eukaryotic cilia and flagella. *Essays Biochem.* **62**, 829–838 (2018).
9. Margulis, L., Chapman, M., Guerrero, R. & Hall, J. The last eukaryotic common ancestor (LECA): acquisition of cytoskeletal motility from aerotolerant spirochetes in the Proterozoic Eon. *Proc. Natl Acad. Sci. USA* **103**, 13080–13085 (2006).
10. Mitchison, T. & Mitchison, H. Cell biology: How cilia beat. *Nature* **463**, 308–309 (2010).
11. Satir, P. & Christensen, S. T. Overview of structure and function of mammalian cilia. *Annu. Rev. Physiol.* **69**, 377–400 (2007).
12. Gray, J. The mechanism of ciliary movement.—VI. Photographic and stroboscopic analysis of ciliary movement. *Proc. R. Soc. Lond. B* **107**, 313–332 (1930).
13. Machin, K. E. The control and synchronization of flagellar movement. *Proc. R. Soc. Lond. B* **158**, 88–104 (1963).
14. Blake, J. R. & Sleigh, M. A. Mechanics of ciliary locomotion. *Biol. Rev.* **49**, 85–125 (1974).
15. Blake, J. R. & Chwang, A. T. Fundamental singularities of viscous flow. *J. Eng. Math.* **8**, 23–29 (1974).
16. Gray, J. & Hancock, G. J. The propulsion of sea-urchin spermatozoa. *J. Exp. Biol.* **32**, 802–814 (1955).
17. Hand, W. G. & Haupt, W. Flagellar activity of the colony members of *Volvox aureus* Ehrbg. during light stimulation. *J. Protozool.* **18**, 361–364 (1971).
18. Sleigh, M. A. The form of beat in cilia of *Stentor* and *Opalina*. *J. Exp. Biol.* **37**, 1–10 (1960).
19. Schwartz, E. A., Leonard, M. L., Bizios, R. & Bowser, S. S. Analysis and modeling of the primary cilium bending response to fluid shear. *Am. J. Physiol. Ren. Physiol.* **272**, F132–F138 (1997).
20. Wiggins, C. H. & Goldstein, R. E. Flexive and propulsive dynamics of elastica at low Reynolds number. *Phys. Rev. Lett.* **80**, 3879 (1998).
21. Camalet, S. & Jülicher, F. Generic aspects of axonemal beating. *N. J. Phys.* **2**, 24 (2000).
22. Xu, G. et al. Flexural rigidity and shear stiffness of flagella estimated from induced bends and counterbends. *Biophys. J.* **110**, 2759–2768 (2016).
23. Bandyopadhyay, P. R. & Hansen, J. C. Breakup and then makeup: a predictive model of how cilia self-regulate hardness for posture control. *Sci. Rep.* **3**, 1956 (2013).
24. Chen, D. T., Heymann, M., Fraden, S., Nicastro, D. & Dogic, Z. ATP consumption of eukaryotic flagella measured at a single-cell level. *Biophys. J.* **109**, 2562–2573 (2015).
25. Lindemann, C. B. Structural-functional relationships of the dynein, spokes, and central-pair projections predicted from an analysis of the forces acting within a flagellum. *Biophys. J.* **84**, 4115–4126 (2003).
26. Jülicher, F., Ajdari, A. & Prost, J. Modeling molecular motors. *Rev. Mod. Phys.* **69**, 1269 (1997).
27. Lindemann, C. B. A "geometric clutch" hypothesis to explain oscillations of the axoneme of cilia and flagella. *J. Theor. Biol.* **168**, 175–189 (1994).
28. Brokaw, C. J. Molecular mechanism for oscillation in flagella and muscle. *Proc. Natl Acad. Sci. USA* **72**, 3102–3106 (1975).
29. Elgeti, J., Winkler, R. G. & Gompper, G. Physics of microswimmers: single particle motion and collective behavior: a review. *Rep. Prog. Phys.* **78**, 056601 (2015).
30. Vernon, G. G. & Woolley, D. M. Basal sliding and the mechanics of oscillation in a mammalian sperm flagellum. *Biophys. J.* **87**, 3934–3944 (2004).
31. Riedel-Kruse, I. H., Hilfinger, A., Howard, J. & Jülicher, F. How molecular motors shape the flagellar beat. *HFSP J.* **1**, 192–208 (2007).
32. Lin, J. & Nicastro, D. Asymmetric distribution and spatial switching of dynein activity generates ciliary motility. *Science* **360**, eaar1968 (2018).
33. Brokaw, C. J. & Luck, D. J. L. Bending patterns of *Chlamydomonas* flagella: III. A radial spoke head deficient mutant and a central pair deficient mutant. *Cell Motil.* **5**, 195–208 (1985).
34. Sartori, P., Geyer, V. F., Scholich, A., Jülicher, F. & Howard, J. Dynamic curvature regulation accounts for the symmetric and asymmetric beats of chlamydomonas flagella. *eLife* **5**, e13258 (2016).
35. Hilfinger, A., Chattopadhyay, A. K. & Jülicher, F. Nonlinear dynamics of cilia and flagella. *Phys. Rev. E* **79**, 051918 (2009).
36. Ishimoto, K. & Gaffney, E. A. An elastohydrodynamical simulation study of filament and spermatozoan swimming driven by internal couples. *IMA J. Appl. Math.* **83**, 655–679 (2018).

37. Laskar, A. et al. Hydrodynamic instabilities provide a generic route to spontaneous biomimetic oscillations in chemomechanically active filaments. *Sci. Rep.* **3**, 1964 (2013).
38. Lacey, S. E., He, S., Scheres, S. H. W. & Carter, A. P. Cryo-EM of dynein microtubule-binding domains shows how an axonemal dynein distorts the microtubule. *eLife* **8**, e47145 (2019).
39. Ferreira, R. R., Vilfan, A., Jülicher, F., Supatto, W. & Vermot, J. Physical limits of flow sensing in the left-right organizer. *eLife* **6**, e25078 (2017).
40. Chaaban, S. & Brouhard, G. J. A microtubule bestiary: structural diversity in tubulin polymers. *Mol. Biol. Cell* **28**, 2924–2931 (2017).
41. Friedrich, B. Hydrodynamic synchronization of flagellar oscillators. *Eur. Phys. J. Spec. Top.* **225**, 2353–2368 (2016).
42. Klindt, G. S., Ruloff, C., Wagner, C. & Friedrich, B. M. Load response of the flagellar beat. *Phys. Rev. Lett.* **117**, 258101 (2016).
43. Okuno, M. & Hiramoto, Y. Mechanical stimulation of starfish sperm flagella. *J. Exp. Biol.* **65**, 401–413 (1976).
44. Hill, D. B. et al. Force generation and dynamics of individual cilia under external loading. *Biophys. J.* **98**, 57–66 (2010).
45. Machemer, H. Ciliary activity and the origin of metachrony in paramecium: effects of increased viscosity. *J. Exp. Biol.* **57**, 239–259 (1972).
46. Gheber, L., Korngreen, A. & Priel, Z. Effect of viscosity on metachrony in mucus propelling cilia. *Cell Motil. Cytoskelet.* **39**, 9–20 (1998).
47. Shingyoji, C., Higuchi, H., Yoshimura, M., Katayama, E. & Yanagida, T. Dynein arms are oscillating force generators. *Nature* **393**, 711–714 (1998).
48. Jülicher, F. & Prost, J. Spontaneous oscillations of collective molecular motors. *Phys. Rev. Lett.* **78**, 4510 (1997).
49. Eshel, D., Grossman, Y. & Priel, Z. Spectral characterization of ciliary beating: variations of frequency with time. *Am. J. Physiol. Cell Physiol.* **249**, C160–C165 (1985).
50. Ma, R., Klindt, G. S., Riedel-Kruse, I. H., Jülicher, F. & Friedrich, B. M. Active phase and amplitude fluctuations of flagellar beating. *Phys. Rev. Lett.* **113**, 048101 (2014).
51. Wan, K. Y. & Goldstein, R. E. Rhythmicity, recurrence, and recovery of flagellar beating. *Phys. Rev. Lett.* **113**, 238103 (2014).
52. Han, J. & Peskin, C. S. Spontaneous oscillation and fluid–structure interaction of cilia. *Proc. Natl Acad. Sci. USA* **115**, 4417–4422 (2018).
53. Gadêlha, H., Gaffney, E., Smith, D. & Kirkman-Brown, J. Nonlinear instability in flagellar dynamics: a novel modulation mechanism in sperm migration? *J. R. Soc. Interface* **7**, 1689–1697 (2010).
54. Bayly, P. V. & Dutcher, S. K. Steady dynein forces induce flutter instability and propagating waves in mathematical models of flagella. *J. R. Soc. Interface* **13**, 20160523 (2016).
55. Hu, T. & Bayly, P. V. Finite element models of flagella with sliding radial spokes and interdoublet links exhibit propagating waves under steady dynein loading. *Cytoskeleton* **75**, 185–200 (2018).
56. Ling, F., Guo, H. & Kanso, E. Instability-driven oscillations of elastic microfilaments. *J. R. Soc. Interface* **15**, 20180594 (2018).
57. Bottier, M., Thomas, K. A., Dutcher, S. K. & Bayly, P. V. How does cilium length affect beating? *Biophys. J.* **116**, 1292–1304 (2019).
58. Gray, J. *Ciliary Movement. Cambridge Comparative Physiology* (Cambridge Univ. Press, 1928).
59. Rothschild. Measurement of sperm activity before artificial insemination. *Nature* **163**, 358–359 (1949).
60. Riedel, I. H., Kruse, K. & Howard, J. A self-organized vortex array of hydrodynamically entrained sperm cells. *Science* **309**, 300–303 (2005).
61. Quaranta, G., Aubin-Tam, M.-E. & Tam, D. Hydrodynamics versus intracellular coupling in the synchronization of eukaryotic flagella. *Phys. Rev. Lett.* **115**, 238101 (2015).
62. Wan, K. Y. & Goldstein, R. E. Coordinated beating of algal flagella is mediated by basal coupling. *Proc. Natl Acad. Sci. USA* **113**, E2784–E2793 (2016).
63. Brumley, D. R., Wan, K. Y., Polin, M. & Goldstein, R. E. Flagellar synchronization through direct hydrodynamic interactions. *eLife* **3**, e02750 (2014).
64. Gueron, S., Levit-Gurevich, K., Liron, N. & Blum, J. J. Cilia internal mechanism and metachronal coordination as the result of hydrodynamical coupling. *Proc. Natl Acad. Sci. USA* **94**, 6001–6006 (1997).
65. Niedermayer, T., Eckhardt, B. & Lenz, P. Synchronization, phase locking, and metachronal wave formation in ciliary chains. *Chaos* **18**, 037128 (2008).
66. Vilfan, A. & Jülicher, F. Hydrodynamic flow patterns and synchronization of beating cilia. *Phys. Rev. Lett.* **96**, 058102 (2006).
67. Pikovsky, A., Rosenblum, M., Kurths, J. & Kurths, J. *Synchronization: A Universal Concept in Nonlinear Sciences* Vol. 12 (Cambridge Univ. Press, 2003).
68. Guo, H., Fauci, L., Shelley, M. & Kanso, E. Bistability in the synchronization of actuated microfilaments. *J. Fluid Mech.* **836**, 304–323 (2018).
69. Kim, Y. W. & Netz, R. R. Pumping fluids with periodically beating grafted elastic filaments. *Phys. Rev. Lett.* **96**, 158101 (2006).
70. Coy, R. & Gadêlha, H. The counterbend dynamics of cross-linked filament bundles and flagella. *J. R. Soc. Interface* **14**, 20170065 (2017).
71. Lindemann, C. B., Macauley, L. J. & Lesich, K. A. The counterbend phenomenon in dynein-disabled rat sperm flagella and what it reveals about the interdoublet elasticity. *Biophys. J.* **89**, 1165–1174 (2005).
72. Goldstein, R. E. Green algae as model organisms for biological fluid dynamics. *Annu. Rev. Fluid Mech.* **47**, 343–375 (2015).
73. Goldstein, R. E., Polin, M. & Tuval, I. Noise and synchronization in pairs of beating eukaryotic flagella. *Phys. Rev. Lett.* **103**, 168103 (2009).
74. Wan, K. Y., Leptos, K. C. & Goldstein, R. E. Lag, lock, sync, slip: the many 'phases' of coupled flagella. *J. R. Soc. Interface* **11**, 20131160 (2014).
75. Geyer, V. F., Jülicher, F., Howard, J. & Friedrich, B. M. Cell-body rocking is a dominant mechanism for flagellar synchronization in a swimming alga. *Proc. Natl Acad. Sci. USA* **110**, 18058–18063 (2013).
76. Elfring, G. J. & Lauga, E. Hydrodynamic phase locking of swimming microorganisms. *Phys. Rev. Lett.* **103**, 088101 (2009).
77. Friedrich, B. M. & Jülicher, F. Flagellar synchronization independent of hydrodynamic interactions. *Phys. Rev. Lett.* **109**, 138102 (2012).
78. Lauga, E. & Powers, T. R. The hydrodynamics of swimming microorganisms. *Rep. Prog. Phys.* **72**, 096601 (2009).
79. Goldstein, R. E. *Batchelor Prize Lecture* Fluid dynamics at the scale of the cell. *J. Fluid Mech.* **807**, 1–39 (2016).
80. Tam, D. & Hosoi, A. Optimal feeding and swimming gaits of biflagellated organisms. *Proc. Natl Acad. Sci. USA* **108**, 1001–1006 (2011).
81. Wan, K. Y. et al. Reorganisation of complex ciliary flows around regenerating *Stentor coeruleus*. Preprint at *bioRxiv* https://doi.org/10.1101/681908 (2019).
82. Polin, M., Tuval, I., Drescher, K., Gollub, J. P. & Goldstein, R. E. Chlamydomonas swims with two gears in a eukaryotic version of run-and-tumble locomotion. *Science* **325**, 487–490 (2009).
83. Rüffer, U. & Nultsch, W. Comparison of the beating of cis- and trans-flagella of *Chlamydomonas* cells held on micropipettes. *Cell Motil. Cytoskelet.* **7**, 87–93 (1987).
84. Wan, K. Y. & Goldstein, R. E. Time irreversibility and criticality in the motility of a flagellate microorganism. *Phys. Rev. Lett.* **121**, 058103 (2018).
85. Kung, C. & Saimi, Y. The physiological basis of taxes in *Paramecium*. *Annu. Rev. Physiol.* **44**, 519–534 (1982).
86. Mathijssen, A. J. T. M., Culver, J., Bhamla, M. S. & Prakash, M. Collective intercellular communication through ultra-fast hydrodynamic trigger waves. *Nature* **571**, 560–564 (2019).
87. Bayless, B. A., Giddings, T. H. Jr, Winey, M. & Pearson, C. G. Bld10/Cep135 stabilizes basal bodies to resist cilia-generated forces. *Mol. Biol. Cell* **23**, 4820–4832 (2012).
88. Coyle, S. M., Flaum, E., Li, H., Krishnamurthy, D. & Prakash, M. Coupled active systems encode an emergent hunting behavior in the unicellular predator *Lacrymaria olor*. *Curr. Biol.* **29**, 3838–3850.e3 (2019).
89. Ainsworth, C. Cilia: tails of the unexpected. *Nature* **448**, 638–641 (2007).
90. Grosberg, R. K. & Strathmann, R. R. The evolution of multicellularity: a minor major transition? *Annu. Rev. Ecol. Evol. Syst.* **38**, 621–654 (2007).
91. Nielsen, C. Six major steps in animal evolution: are we derived sponge larvae? *Evol. Dev.* **10**, 241–257 (2008).
92. Uchida, N. & Golestanian, R. Synchronization and collective dynamics in a carpet of microfluidic rotors. *Phys. Rev. Lett.* **104**, 178103 (2010).
93. King, N. The unicellular ancestry of animal development. *Dev. Cell* **7**, 313–325 (2004).
94. Nielsen, L. T. et al. Hydrodynamics of microbial filter feeding. *Proc. Natl Acad. Sci. USA* **114**, 9373–9378 (2017).
95. Pettitt, M. E., Orme, B. A. A., Blake, J. R. & Leadbeater, B. S. C. The hydrodynamics of filter feeding in choanoflagellates. *Eur. J. Protistol.* **38**, 313–332 (2002).
96. Higdon, J. J. L. The generation of feeding currents by flagellar motions. *J. Fluid Mech.* **94**, 305–330 (1979).
97. Roper, M., Dayel, M. J., Pepper, R. E. & Koehl, M. Cooperatively generated stresslet flows supply fresh fluid to multicellular choanoflagellate colonies. *Phys. Rev. Lett.* **110**, 228104 (2013).
98. Orme, B. A. A., Otto, S. R. & Blake, J. R. Chaos and mixing in micro-biological fluid dynamics: blinking stokeslets. *Math. Methods Appl. Sci.* **24**, 1337–1349 (2001).
99. Kirkegaard, J. B., Marron, A. O. & Goldstein, R. E. Motility of colonial choanoflagellates and the statistics of aggregate random walkers. *Phys. Rev. Lett.* **116**, 038102 (2016).
100. Kirkegaard, J. B., Bouillant, A., Marron, A. O., Leptos, K. C. & Goldstein, R. E. Aerotaxis in the closest relatives of animals. *eLife* **5**, e18109 (2016).
101. Bidder, G. P. The relation of the form of a sponge to its currents. *Q. J. Microsc. Sci.* **67**, 293–323 (1923).
102. Reiswig, H. M. Water transport, respiration and energetics of three tropical marine sponges. *J. Exp. Mar. Biol. Ecol.* **14**, 231–249 (1974).
103. Mah, J. L., Christensen-Dalsgaard, K. K. & Leys, S. P. Choanoflagellate and choanocyte collar-flagellar systems and the assumption of homology. *Evol. Dev.* **16**, 25–37 (2014).
104. Sogabe, S. et al. Pluripotency and the origin of animal multicellularity. *Nature* **570**, 519–522 (2019).
105. LaBarbera, M. Principles of design of fluid transport systems in zoology. *Science* **249**, 992–1000 (1990).
106. Asadzadeh, S. S., Larsen, P. S., Riisgård, H. U. & Walther, J. H. Hydrodynamics of the leucon sponge pump. *J. R. Soc. Interface* **16**, 20180630 (2019).
107. Shapiro, O. H. et al. Vortical ciliary flows actively enhance mass transport in reef corals. *Proc. Natl Acad. Sci. USA* **111**, 13391–13396 (2014).
108. Armon, S., Bull, M. S., Aranda-Diaz, A. & Prakash, M. Ultrafast epithelial contractions provide insights into contraction speed limits and tissue integrity. *Proc. Natl Acad. Sci. USA* **115**, E10333–E10341 (2018).
109. Prakash, V., Bull, M. S. & Prakash, M. Motility induced fracture reveals a ductile to brittle crossover in the epithelial tissues of a simple animal. Preprint at *bioRxiv* https://doi.org/10.1101/676866 (2019).
110. Smith, C. L., Reese, T. S., Govezensky, T. & Barrio, R. A. Coherent directed movement toward food modeled in *Trichoplax*, a ciliated animal lacking a nervous system. *Proc. Natl Acad. Sci. USA* **116**, 8901–8908 (2019).
111. Smith, C. L., Pivovarova, N. & Reese, T. S. Coordinated feeding behavior in *Trichoplax*, an animal without synapses. *PLOS ONE* **10**, e0136098 (2015).
112. Varoqueaux, F. et al. High cell diversity and complex peptidergic signaling underlie placozoan behavior. *Curr. Biol.* **28**, 3495–3501 (2018).
113. Emlet, R. B. Functional constraints on the evolution of larval forms of marine invertebrates: experimental and comparative evidence. *Am. Zool.* **31**, 707–725 (1991).
114. Bick, C., Goodfellow, M., Laing, C. R. & Martens, E. A. Understanding the dynamics of biological and neural oscillator networks through mean-field reductions: a review. Preprint at *arXiv* https://arxiv.org/abs/1902.05307 (2019).
115. Panaggio, M. J. & Abrams, D. M. Chimera states: coexistence of coherence and incoherence in networks of coupled oscillators. *Nonlinearity* **28**, R67 (2015).
116. Jékely, G. Origin and early evolution of neural circuits for the control of ciliary locomotion. *Proc. R. Soc. B* **278**, 914–922 (2010).
117. Bezares-Calderon, L. A. et al. Neural circuitry of a polycystin-mediated hydrodynamic startle response for predator avoidance. *eLife* **7**, e36262 (2018).
118. Verasztó, C. et al. Ciliomotor circuitry underlying whole-body coordination of ciliary activity in the *Platynereis* larva. *eLife* **6**, e26000 (2017).
119. Lenz, P. & Ryskin, A. Collective effects in ciliar arrays. *Phys. Biol.* **3**, 285 (2006).
120. Leoni, M. & Liverpool, T. B. Hydrodynamic synchronization of nonlinear oscillators at low Reynolds number. *Phys. Rev. E* **85**, 040901 (2012).

121. Guirao, B. & Joanny, J.-F. Spontaneous creation of macroscopic flow and metachronal waves in an array of cilia. *Biophys. J.* **92**, 1900–1917 (2007).
122. Knight-Jones, E. W. Relations between metachronism and the direction of ciliary beat in metazoa. *J. Cell Sci.* **3**, 503–521 (1954).
123. Sleigh, M. A., Blake, J. R. & Liron, N. The propulsion of mucus by cilia. *Am. Rev. Respir. Dis.* **137**, 726–741 (1988).
124. Elgeti, J. & Gompper, G. Emergence of metachronal waves in cilia arrays. *Proc. Natl Acad. Sci. USA* **110**, 4470–4475 (2013).
125. Babataheri, A., Roper, M., Fermigier, M. & Du Roure, O. Tethered fleximags as artificial cilia. *J. Fluid Mech.* **678**, 5–13 (2011).
126. Shields, A. R. et al. Biomimetic cilia arrays generate simultaneous pumping and mixing regimes. *Proc. Natl Acad. Sci. USA* **107**, 15670–15675 (2010).
127. Hanasoge, S., Hesketh, P. J. & Alexeev, A. Microfluidic pumping using artificial magnetic cilia. *Microsyst. Nanoeng.* **4**, 11 (2018).
128. Gheber, L. & Priel, Z. Ciliary activity under normal conditions and under viscous load. *Biorheology* **27**, 547–557 (1990).
129. Guo, H. & Kanso, E. Evaluating efficiency and robustness in cilia design. *Phys. Rev. E* **93**, 033119 (2016).
130. Smith, D. J., Gaffney, E. A. & Blake, J. R. Modelling mucociliary clearance. *Respir. Physiol. Neurobiol.* **163**, 178–188 (2008).
131. Osterman, N. & Vilfan, A. Finding the ciliary beating pattern with optimal efficiency. *Proc. Natl Acad. Sci. USA* **108**, 15727–15732 (2011).
132. Guo, H., Nawroth, J., Ding, Y. & Kanso, E. Cilia beating patterns are not hydrodynamically optimal. *Phys. Fluids* **26**, 091901 (2014).
133. Spagnolie, S. E. & Lauga, E. The optimal elastic flagellum. *Phys. Fluids* **22**, 031901 (2010).
134. Gueron, S. & Levit-Gurevich, K. Energetic considerations of ciliary beating and the advantage of metachronal coordination. *Proc. Natl Acad. Sci. USA* **96**, 12240–12245 (1999).
135. Chateau, S., Favier, J., D'ortona, U. & Poncet, S. Transport efficiency of metachronal waves in 3D cilium arrays immersed in a two-phase flow. *J. Fluid Mech.* **824**, 931–961 (2017).
136. Datt, C., Natale, G., Hatzikiriakos, S. G. & Elfring, G. J. An active particle in a complex fluid. *J. Fluid Mech.* **823**, 675–688 (2017).
137. Brokaw, C. J. & Simonick, T. F. Mechanochemical coupling in flagella. V. Effects of viscosity on movement and ATP-dephosphorylation of Triton-demembranated sea-urchin spermatozoa. *J. Cell Sci.* **23**, 227–241 (1977).
138. Mettot, C. & Lauga, E. Energetics of synchronized states in three-dimensional beating flagella. *Phys. Rev. E* **84**, 061905 (2011).
139. Ding, Y., Nawroth, J. C., McFall-Ngai, M. J. & Kanso, E. Mixing and transport by ciliary carpets: a numerical study. *J. Fluid Mech.* **743**, 124–140 (2014).
140. Blake, J. A model for the micro-structure in ciliated organisms. *J. Fluid Mech.* **55**, 1–23 (1972).
141. Smith, D. J., Gaffney, E. A. & Blake, J. R. Discrete cilia modelling with singularity distributions: application to the embryonic node and the airway surface liquid. *Bull. Math. Biol.* **69**, 1477–1510 (2007).
142. Quek, R., Lim, K. M. & Chiam, K. H. *Three-Dimensional Simulations of Ciliary Flow* 197–218 (Springer, 2014).
143. Supatto, W., Fraser, S. E. & Vermot, J. An all-optical approach for probing microscopic flows in living embryos. *Biophys. J.* **95**, L29–L31 (2008).
144. Ramirez-San Juan, G. R. et al. Multi-scale spatial heterogeneity enhances particle clearance in airway ciliary arrays. Preprint at *bioRxiv* https://doi.org/10.1101/665125 (2019).
145. Schneiter, M., Ricka, J. & Frenz, M. Self-organization of self-clearing beating patterns in an array of locally interacting ciliated cells formulated as an adaptive boolean network. *Theory Biosci.* https://doi.org/10.1007/s12064-019-00299-x (2019).
146. Faubel, R., Westendorf, C., Bodenschatz, E. & Eichele, G. Cilia-based flow network in the brain ventricles. *Science* **353**, 176–178 (2016).
147. Veening, J. G. & Barendregt, H. P. The regulation of brain states by neuroactive substances distributed via the cerebrospinal fluid; a review. *Cerebrospinal Fluid Res.* **7**, 1 (2010).
148. Pellicciotta, N. et al. Synchronization of mammalian motile cilia in the brain with hydrodynamic forces. Preprint at *bioRxiv* https://doi.org/10.1101/668459 (2019).
149. Devenport, D. The cell biology of planar cell polarity. *J. Cell Biol.* **207**, 171–179 (2014).
150. Vladar, E. K., Lee, Y. L., Stearns, T. & Axelrod, J. D. in *Methods in Cell Biology* Vol. 127 Ch. 3 (eds Basto, R. & Marshall, W. F.) 37–54 (Elsevier, 2015).
151. Hilfinger, A. & Jülicher, F. The chirality of ciliary beats. *Phys. Biol.* **5**, 016003 (2008).
152. Kim, M. J. & Breuer, K. S. Microfluidic pump powered by self-organizing bacteria. *Small* **4**, 111–118 (2008).
153. Mathijssen, A. J., Guzmán-Lastra, F., Kaiser, A. & Löwen, H. Nutrient transport driven by microbial active carpets. *Phys. Rev. Lett.* **121**, 248101 (2018).
154. Golestanian, R., Yeomans, J. M. & Uchida, N. Hydrodynamic synchronization at low Reynolds number. *Soft Matter* **7**, 3074–3082 (2011).
155. Uchida, N., Golestanian, R. & Bennett, R. R. Synchronization and collective dynamics of flagella and cilia as hydrodynamically coupled oscillators. *J. Phys. Soc. Jpn.* **86**, 101007 (2017).
156. Brumley, D. R. et al. Long-range interactions, wobbles, and phase defects in chains of model cilia. *Phys. Rev. Fluids* **1**, 081201 (2016).
157. Solon, A. & Tailleur, J. Revisiting the flocking transition using active spins. *Phys. Rev. Lett.* **111**, 078101 (2013).
158. Gilpin, W., Prakash, V. N. & Prakash, M. Vortex arrays and ciliary tangles underlie the feeding–swimming trade-off in starfish larvae. *Nat. Phys.* **13**, 380–386 (2017).
159. Bourland, W. A., Wendell, L., Hampikian, G. & Vdancỳ, P. Morphology and phylogeny of *Bryophryoides ocellatus* ng, n. sp.(Ciliophora, Colpodea) from in situ soil percolates of Idaho, USA. *Eur. J. Protistol.* **50**, 47–67 (2014).
160. Feriani, L. et al. Assessing the collective dynamics of motile cilia in cultures of human airway cells by multiscale DDM. *Biophys. J.* **113**, 109–119 (2017).
161. Brumley, D. R., Polin, M., Pedley, T. J. & Goldstein, R. E. Metachronal waves in the flagellar beating of *Volvox* and their hydrodynamic origin. *J. R. Soc. Interface* **12**, 20141358 (2015).
162. Nielsen, C. Structure and function of metazoan ciliary bands and their phylogenetic significance. *Acta Zool.* **68**, 205–262 (1987).
163. Strathmann, R. R. The evolution and loss of feeding larval stages of marine invertebrates. *Evolution* **32**, 894–906 (1978).
164. Agassiz, A. *North American Starfishes* Vol. 5 (Welch, Bigelow, and Company, Univ. Press, 1877).
165. Riisgård, H. U. & Larsen, P. S. Minireview: Ciliary filter feeding and bio-fluid mechanics—present understanding and unsolved problems. *Limnol. Oceanogr.* **46**, 882–891 (2001).
166. Jorgensen, C. B. Fluid mechanical aspects of suspension feeding. *Mar. Ecol. Prog. Ser.* **11**, 89–103 (1983).
167. Rubenstein, D. I. & Koehl, M. A. R. The mechanisms of filter feeding: some theoretical considerations. *Am. Naturalist* **111**, 981–994 (1977).
168. Mathijssen, A. J., Jeanneret, R. & Polin, M. Universal entrainment mechanism controls contact times with motile cells. *Phys. Rev. Fluids* **3**, 033103 (2018).
169. Ding, Y. & Kanso, E. Selective particle capture by asynchronously beating cilia. *Phys. Fluids* **27**, 121902 (2015).
170. Gilpin, W., Prakash, V. N. & Prakash, M. Dynamic vortex arrays created by starfish larvae. *Phys. Rev. Fluids* **2**, 090501 (2017).
171. Gilpin, W., Prakash, V. N. & Prakash, M. Rapid behavioral transitions produce chaotic mixing by a planktonic microswimmer. Preprint at *arXiv* https://arxiv.org/abs/1804.08773 (2018).
172. Gilpin, W., Prakash, V. N. & Prakash, M. Flowtrace: simple visualization of coherent structures in biological fluid flows. *J. Exp. Biol.* **220**, 3411–3418 (2017).
173. von Dassow, G., Emlet, R. & Grünbaum, D. Boundary effects on currents around ciliated larvae. *Nat. Phys.* **13**, 520–521 (2017).
174. Gilpin, W., Prakash, V. N. & Prakash, M. Reply to 'Boundary effects on currents around ciliated larvae'. *Nat. Phys.* **13**, 521–522 (2017).
175. Krishnamurthy, D. et al. Scale-free vertical tracking microscopy: Towards bridging scales in biological oceanography. Preprint at *bioRxiv* https://doi.org/10.1101/610246 (2019).
176. Bruot, N. & Cicuta, P. Realizing the physics of motile cilia synchronization with driven colloids. *Annu. Rev. Condens. Matter Phys.* **7**, 323–348 (2016).
177. Amemiya, S. et al. Development of ciliary bands in larvae of the living isocrinid sea lily *Metacrinus rotundus*. *Acta Zool.* **96**, 36–43 (2015).
178. Nasouri, B. & Elfring, G. J. Hydrodynamic interactions of cilia on a spherical body. *Phys. Rev. E* **93**, 033111 (2016).
179. Ghorbani, A. & Najafi, A. Symplectic and antiplectic waves in an array of beating cilia attached to a closed body. *Phys. Rev. E* **95**, 052412 (2017).
180. Panaggio, M. J. & Abrams, D. M. Chimera states on a flat torus. *Phys. Rev. Lett.* **110**, 094102 (2013).
181. Kuramoto, Y. & Battogtokh, D. Coexistence of coherence and incoherence in nonlocally coupled phase oscillators. *Nonlinear Phenom. Complex Syst.* **5**, 380–385 (2002).
182. Abrams, D. M. & Strogatz, S. H. Chimera states for coupled oscillators. *Phys. Rev. Lett.* **93**, 174102 (2004).
183. Wollin, C. & Stark, H. Metachronal waves in a chain of rowers with hydrodynamic interactions. *Eur. Phys. J. E* **34**, 42 (2011).
184. Nawroth, J. C. et al. Motile cilia create fluid-mechanical microhabitats for the active recruitment of the host microbiome. *Proc. Natl Acad. Sci. USA* **114**, 9510–9516 (2017).
185. Childress, S. & Dudley, R. Transition from ciliary to flapping mode in a swimming mollusc: flapping flight as a bifurcation in Reω. *J. Fluid Mech.* **498**, 257–288 (2004).
186. Reiten, I. et al. Motile-cilia-mediated flow improves sensitivity and temporal resolution of olfactory computations. *Curr. Biol.* **27**, 166–174 (2017).
187. Pfeifer, R., Lungarella, M. & Iida, F. Self-organization, embodiment, and biologically inspired robotics. *Science* **318**, 1088–1093 (2007).
188. Mohren, T. L., Daniel, T. L., Brunton, S. L. & Brunton, B. W. Neural-inspired sensors enable sparse, efficient classification of spatiotemporal data. *Proc. Natl Acad. Sci. USA* **115**, 10564–10569 (2018).
189. Hauser, H., Ijspeert, A. J., Füchslin, R. M., Pfeifer, R. & Maass, W. Towards a theoretical foundation for morphological computation with compliant bodies. *Biol. Cybern.* **105**, 355–370 (2011).
190. Mayne, R. & den Toonder, J. *Atlas of Cilia Bioengineering and Biocomputing* (River Publishers, 2018).
191. Guérin, T., Prost, J. & Joanny, J.-F. Dynamical behavior of molecular motor assemblies in the rigid and crossbridge models. *Eur. Phys. J. E* **34**, 60 (2011).
192. Guérin, T., Prost, J. & Joanny, J.-F. Bidirectional motion of motor assemblies and the weak-noise escape problem. *Phys. Rev. E* **84**, 041901 (2011).
193. Van Kampen, N. G. *Stochastic Processes in Physics and Chemistry* Vol. 1 (Elsevier, 1992).
194. Uchida, N. & Golestanian, R. Generic conditions for hydrodynamic synchronization. *Phys. Rev. Lett.* **106**, 058104 (2011).
195. Mirzakhanloo, M. & Alam, M.-R. Flow characteristics of chlamydomonas result in purely hydrodynamic scattering. *Phys. Rev. E* **98**, 012603 (2018).
196. Wei, D., Dehnavi, P. G., Aubin-Tam, M.-E. & Tam, D. Is the zero Reynolds number approximation valid for ciliary flows? *Phys. Rev. Lett.* **122**, 124502 (2019).
197. Hong, H. & Strogatz, S. H. Kuramoto model of coupled oscillators with positive and negative coupling parameters: an example of conformist and contrarian oscillators. *Phys. Rev. Lett.* **106**, 054102 (2011).
198. Zakharova, A., Kapeller, M. & Schöll, E. Chimera death: symmetry breaking in dynamical networks. *Phys. Rev. Lett.* **112**, 154101 (2014).
199. Gilpin, W. Self-organized avalanches in globally-coupled phase oscillators. Preprint at *arXiv* https://arxiv.org/abs/1906.05514 (2019).
200. Kawamura, Y. Chimera Ising walls in forced nonlocally coupled oscillators. *Phys. Rev. E* **75**, 056204 (2007).
201. Ottino-Löffler, B. & Strogatz, S. H. Volcano transition in a solvable model of frustrated oscillators. *Phys. Rev. Lett.* **120**, 264102 (2018).
202. Abrams, D. M., Mirollo, R., Strogatz, S. H. & Wiley, D. A. Solvable model for chimera states of coupled oscillators. *Phys. Rev. Lett.* **101**, 084103 (2008).
203. Totz, J. F., Rode, J., Tinsley, M. R., Showalter, K. & Engel, H. Spiral wave chimera states in large populations of coupled chemical oscillators. *Nat. Phys.* **14**, 282–285 (2018).
204. Brumley, D. R., Polin, M., Pedley, T. J. & Goldstein, R. E. Hydrodynamic synchronization and metachronal waves on the surface of the colonial alga *Volvox carteri*. *Phys. Rev. Lett.* **109**, 268102 (2012).
205. Kotar, J. et al. Optimal hydrodynamic synchronization of colloidal rotors. *Phys. Rev. Lett.* **111**, 228103 (2013).
206. Dreyfus, R. et al. Microscopic artificial swimmers. *Nature* **437**, 862–865 (2005).

207. Darnton, N., Turner, L., Breuer, K. & Berg, H. C. Moving fluid with bacterial carpets. *Biophys. J.* **86**, 1863–1870 (2004).
208. Wadhwa, N., Phillips, R. & Berg, H. C. Torque-dependent remodeling of the bacterial flagellar motor. *Proc. Natl Acad. Sci. USA* **116**, 11764–11769 (2019).
209. Sanchez, T., Welch, D., Nicastro, D. & Dogic, Z. Cilia-like beating of active microtubule bundles. *Science* **333**, 456–459 (2011).
210. Sanchez, T., Chen, D. T. N., DeCamp, S. J., Heymann, M. & Dogic, Z. Spontaneous motion in hierarchically assembled active matter. *Nature* **491**, 431–434 (2012).
211. DiPetrillo, C. G. & Smith, E. F. Pcdp1 is a central apparatus protein that binds Ca^{2+}-calmodulin and regulates ciliary motility. *J. Cell Biol.* **189**, 601–612 (2010).
212. Lin, J., Heuser, T., Song, K., Fu, X. & Nicastro, D. One of the nine doublet microtubules of eukaryotic flagella exhibits unique and partially conserved structures. *PLOS ONE* **7**, e46494 (2012).
213. Shoemark, A. & Hogg, C. Electron tomography of respiratory cilia. *Thorax* **68**, 190–191 (2013).
214. Odate, T., Takeda, S., Narita, K. & Kawahara, T. 9+0 and 9+2 cilia are randomly dispersed in the mouse node. *Microscopy* **65**, 119–126 (2016).
215. Wilkerson, C. G., King, S. M., Koutoulis, A., Pazour, G. J. & Witman, G. B. The 78,000 M(r) intermediate chain of Chlamydomonas outer arm dynein is a WD-repeat protein required for arm assembly. *J. Cell Biol.* **129**, 169–178 (1995).
216. Austin-Tse, C. et al. Zebrafish ciliopathy screen plus human mutational analysis identifies C21orf59 and CCDC65 defects as causing primary ciliary dyskinesia. *Am. J. Hum. Genet.* **93**, 672–686 (2013).
217. Stokes, M. Larval locomotion of the lancelet. *J. Exp. Biol.* **200**, 1661–1680 (1997).
218. Bone, Q., Carre, C. & Chang, P. Tunicate feeding filters. *J. Mar. Biol. Assoc. U. K.* **83**, 907–919 (2003).
219. Sutherland, K. R., Madin, L. P. & Stocker, R. Filtration of submicrometer particles by pelagic tunicates. *Proc. Natl Acad. Sci. USA* **107**, 15129–15134 (2010).
220. Petersen, J. K., Mayer, S. & Knudsen, M. Beat frequency of cilia in the branchial basket of the ascidian *Ciona intestinalis* in relation to temperature and algal cell concentration. *Mar. Biol.* **133**, 185–192 (1999).
221. Riisgård, H. U., Nielsen, C. & Larsen, P. S. Downstream collecting in ciliary suspension feeders: the catch-up principle. *Mar. Ecol. Prog. Ser.* **207**, 33–51 (2000).
222. Okabe, N., Xu, B. & Burdine, R. D. Fluid dynamics in zebrafish Kupffer's vesicle. *Dev. Dyn.* **237**, 3602–3612 (2008).

Acknowledgements
The authors thank G. Ramirez-San Juan, A. Mathijssen and the other members of the Prakash Lab for their helpful comments on the manuscript. W.G. was supported by the NSF-Simons Center for Mathematical and Statistical Analysis of Biology at Harvard University, NSF grant no. DMS-1764269, the Harvard FAS Quantitative Biology Initiative, the U. S. Department of Defense National Defense Science and Engineering Graduate (NDSEG) Fellowship Program and the National Geographic Society 'Young Explorers' program. M.S.B. thanks the NSF Graduate Research Fellowship Program and the Stanford Bio-X fellowship. M.P. thanks the NSF Careers Program, NSF 'Center for Cellular Construction' program (DBI-1548297), NIH Directors New Innovator Award, HHMI-Gates Faculty Fellows program, the W. M. Keck Foundation, the Gordon and Betty Moore Foundation and the Chan Zuckerberg Biohub Investigators program for supporting this work.

Author contributions
All authors contributed to the preparation of the manuscript.

Competing interests
The authors declare no competing interests.

Publisher's note
Springer Nature remains neutral with regard to jurisdictional claims in published maps and institutional affiliations.